THE SOUND FIELD AND RADIATION IMPEDANCE OF A HYPERBOLIC HORN

by

Vincent Salmon
A.B., Temple University
1934

M.A., Temple University
1936

Submitted in partial fulfillment of the requirements for the degree of

DOCTOR OF PHILOSOPHY

from the

MASSACHUSETTS INSTITUTE OF TECHNOLOGY

1938

Signature of Author . . . . . .

Department of Physics Dec. 6, 1938

Signature of Professor in Charge of Research

Signature of Chairman of Department Committee on Graduate Students

TABLE OF CONTENTS

ACKNOWLEDGMENTS

It is a pleasure to acknowledge the cheerful co-operation of the Electrical Engineering Department in matters of apparatus and space, as their equipment was used almost exclusively. To Professors Morse and Fay I wish to express my thanks for their helpful criticism and guidance.

ABSTRACT

Of the eleven coordinate systems allowing separable solutions of the wave equation, only the spherical and oblate spheroidal frames have been treated with the definite purpose of using the proper coordinate surface as the boundary of an infinite horn. The last mentioned system produces a horn formed by half a hyperboloid (of revolution) of one sheet, and was investigated by Freehafer.[1] In view of the possibility of checking some of the interesting predictions of the exact theory a hyperbolic horn has been constructed and measurements made of the pressure field and throat impedance. Since the experimental horn did not simulate the infinite one for all frequencies only qualitative agreement with the exact theory was obtained.

In order to take account of the reflected wave, Webster's plane wave assumption has been used as the starting point in the development of a plane wave analysis of general applicability. The results of this analysis are in satisfactory agreement with both exact theory and experimental results for the hyperbolic horn, and indicate that especially for low frequencies the approximate theory will predict with sufficient engineering accuracy the average performance of any reasonably shaped horn.

THE SOUND FIELD AND RADIATION IMPEDANCE OF A HYPERBOLIC HORN

I INTRODUCTION

Among the host of products of modern acoustical research, sound reproducing systems occupy the most prominent place, and to the casual observer the horn from which the radiation proceeds is also visually the most prominent. However, this device has a more important function than that of impressing the listener; and to understand the reasons for using horns a discussion of the details of sound radiation will be not amiss before considering the specific problem indicated by the title of this work. In this introduction, then, we shall briefly consider the wave equation and bring in the concept of acoustical impedance in connection with the radiation from the ideal rigid piston, and then indicate how the need for a horn follows.

If the first order theory is considered, the propagation of acoustic waves of infinitesimal amplitude in a simple fluid medium is represented by

$$\nabla^2 \psi = \frac{\gamma P_0}{\rho_0} \frac{\partial^2 \psi}{\partial t^2} = \frac{1}{C^2} \frac{\partial^2 \psi}{\partial t^2} \qquad (1.1)$$

where ψ is the velocity potential,

γ is the ratio of specific heat at constant pressure to that at constant volume,

P_o is the steady "barometric" pressure,

ρ_o is the steady density of the fluid

and $c^2 = \gamma P_o/\rho_o$ is the wave velocity.

From ψ there may be obtained the particle velocity $\dot{\xi}$ and excess pressure p by[2]

$$\left.\begin{aligned} \dot{\xi} &= -\nabla \psi \\ p &= \rho_o (\partial \psi/\partial t) \end{aligned}\right\} \quad (1.2)$$

These quantities are the departure from the undisturbed and statistically steady conditions; in order for the wave equations to be valid, the amplitude of these quantities must at least be below the auditory threshold of pain, and the waves must traverse not too confined a space.

The radiation of sound is ordinarily accomplished by the communication of the motion of a vibrating surface to the transmitting medium, which we shall take as the atmosphere. According to the method by which the surface is coupled to the air, radiators may be classified as direct or indirect, the latter being formed by a direct radiator plus a horn. Of the former the simplest and most completely worked out practical[3] case is that of a rigid circular plane piston set in a closely fitting hole in an infinite, rigid plane, and oscillating with infinitesimal cisoidal

motion normal to the plane. When the driving force is specified, it is found that with the transmitting medium removed, the relation between force and velocity resulting may be expressed in the form

$$\dot{\xi} = \frac{F}{Z_p} = \frac{F}{R_p + jX_p} \qquad (1.3)$$

Where Z_p is the mechanical impedance of the piston

R_p is the mechanical resistance of the piston

X_p is the mechanical reactance of the piston.

This relation arises directly from the differential equation for the velocity when the time variation is contained in $e^{j\omega t}$. The unit of Z_p is the dyne sec/cm.

Now, when the air is allowed to react back on the piston, the impedance is increased by an amount Z_A, as calculated in the reference cited [3]. This is merely the ratio of the sound pressure integrated over the surface S of the piston, to the velocity $\dot{\xi}$, and may be expressed in the form

$$Z_A = S\rho_o c(r + jx) \qquad (1.4)$$

where the r and x are non-dimensional functions of

$$ka = \frac{2\pi a}{\lambda} = \frac{2\pi a \nu}{c}$$

where a is the piston radius, λ the wavelength and ν the frequency. Thus the essential behaviour of Z_A is represented by r and x; the quantity $S\rho_o c$ gives the dimensions of mechanical impedance to Z_A. The product $\rho_o c$

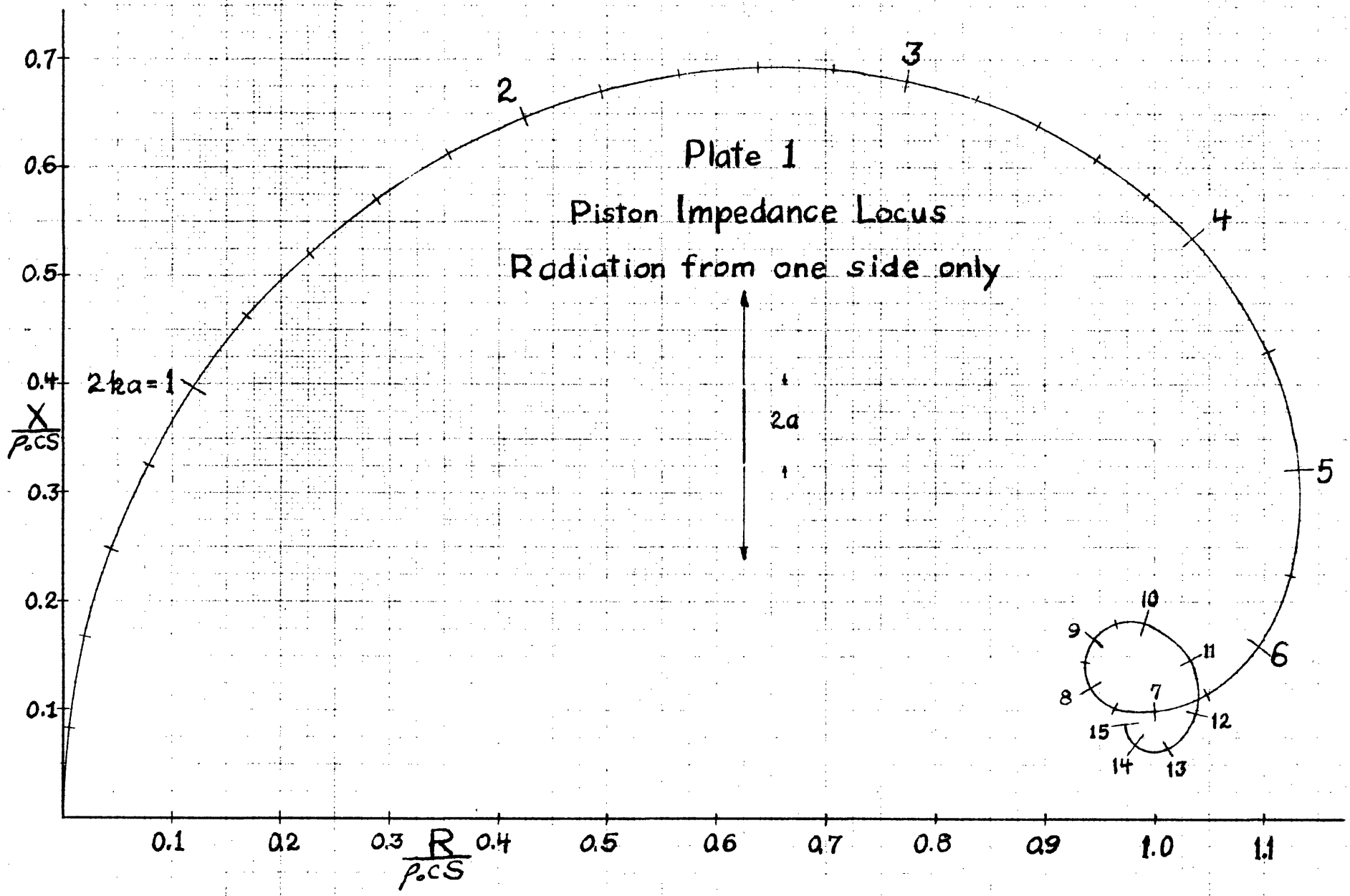
Plate 1
Piston Impedance Locus
Radiation from one side only
2a
2ka=1
2
3
4
5
6
7
8
9
10
11
12
13
14
15
0.1
0.2
0.3
0.4
0.5
0.6
0.7
X/ρcS
R/ρcS
0.1
0.2
0.3
0.4
0.5
0.6
0.7
0.8
0.9
1.0
1.1

is a property of the medium and type of waves[4], and is known as the characteristic impedance of the medium.

The behaviour of Z_A for this piston case is shown in Plate 1, in which r and x are plotted together with the frequency parameter ka determining each point. The important fact to note is that for ka large, or when the product νa is large, the impedance approaches the value $S\rho_0 c + j0$, known as the ultimate impedance. The implications of this behaviour are seen most clearly in considering the amount of sound radiated. From mechanics, the average power is given by the product

$$F_A \dot{\xi}$$

averaged over many periods. Here the complex method fails, so we must use the real parts of the quantities in such an evaluation. With this proviso, and remembering that

$$F_A = \dot{\xi} R_A$$

is the real part of the reaction of the air on the piston, then

$$P_A = \dot{\xi}^2 R_A \qquad (1.5)$$

where P_A is the acoustic power radiated. Thus P_A will not be the same for all frequencies unless the product $\dot{\xi}^2 R_A$ is; and since it is desirable in most cases to obtain this independence of frequency we must examine P_A carefully from the point of view of practical application.

As the practical representative of the rigid piston, the direct radiating, cone type, moving coil loudspeaker is the most common approximation. From the following considerations we proceed to show that it is essentially a low efficiency device. First, most cones cannot be made rigid enough to vibrate as a whole above, say, 800 hz, and greater rigidity is obtained only at the cost of more moving mass, thus limiting the high frequency response. At low frequencies corresponding to $ka < 1$, R_A decreases as the frequency is lowered, and thus the sound power would likewise decrease were it not for the fact that the mechanical resonance of the speaker is placed at the low end of the audio range. Thus the cone velocity will increase (modified by the electrical system), helping to keep the power fairly constant. However, since the moving mass must be large to place the resonant frequency low, most of the mechanical impedance is due to the mass reactance, the radiation resistance R_A contributing but little. Hence most of the electrical input to the moving coil is in the wattless component moving the cone; or, the system is relatively inefficient in that the load is highly reactive. In fact, the electroacoustic transfer efficiency is usually below 5 % over the useful range of frequencies.

To increase this efficiency the solution would be to minimize the moving mass of the piston to such an extent

that the radiation resistance is a large part of the mechanical impedance; or, the acoustic system must obtain its ultimate impedance sooner in frequency. As this latter is only possible for a large piston, and the former only only possible for a small one, the situation demands a means of increasing the apparent size of the piston by loading it in such a fashion that it looks into a system reaching its ultimate impedance quickly, and "reflecting" that impedance, substantially unchanged, back to the actual piston.

It is now fairly easy to visualize the apparatus needed: a horn must be fitted to the piston; and its cross section must increase in such a manner that the "equivalent piston" of the mouth reaches the ultimate impedance quickly, and that this impedance is reflected to the piston. Thus the overall efficiency will be greater, and the output should show less prominent peaks than the simple piston.

The results of this discussion may now be summarized by the statement that the impedance concept is able to suggest the correct design conditions, as well as to interpret the results. In view of the possibility of making a correlated study of a particular horn, we choose the hyperbolic type because of the availability of an exact theory. In the following sections we propose to outline the exact theory due to Freehafer[1], to develop an

approximate theory suitable for calculation and to apply this to the hyperbolic horn, and finally by experiment to obtain results which may be interpreted from both exact and approximate theory. It will be shown that the agreement is satisfactory among the three points of view, and that the approximate theory may be used for calculations of sufficient accuracy to indicate comparative performance.

II EXACT THEORY OF THE HYPERBOLIC HORN

We now consider the results of the theory of the infinite hyperbolic horn; in general, the predictions will be qualitative because the radial functions were not available at the time of this writing. Although the assumption of an infinite horn presents rather difficult experimental conditions, the predictions still should be of general correctness when compared to experiment.

The wave equation for the velocity potential with cisoidal time variation may be written as

$$\nabla^2 \psi + k^2 \psi = 0 \qquad (2.1)$$

(By cisoidal time variation we mean that time is contained in the factor $e^{j\omega t}$). The number of possible solutions of interest to the general horn problem is strictly limited, as the equation is separable in but eleven coordinate systems[5], and still fewer have horn shaped coordinate surfaces. Although Rayleigh has laid the groundwork for the exact treatment of the conical horn[6], to the author's knowledge no complete treatment is yet available, although the functions are rather well known. Hence Freehafer's work is unique in being the first evaluation of a sound field in other than the common geometrical solids.

Turning now to Freehafer's results, we first note the coordinate system, formed by rotating, about the ζ

axis of Fig. 1, families of confocal hyperbolas and ellipses. The figure shows a sample hyperbola,

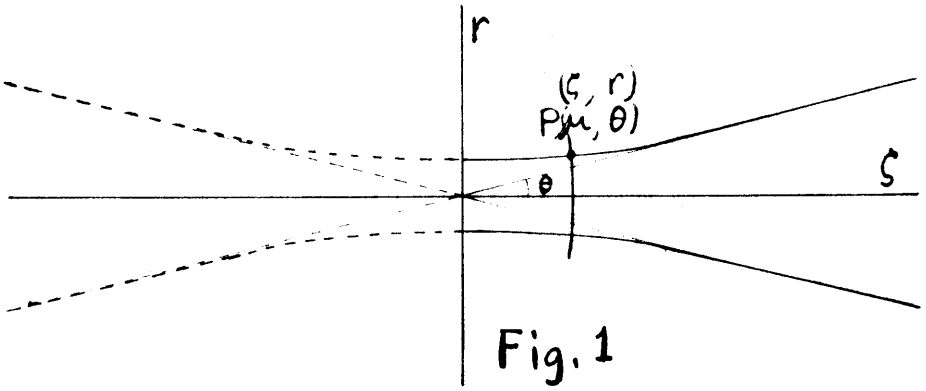

Fig. 1

and its appearance as the profile of a hyperbolic horn, having zero slope at the throat, and approaching asymptotes forming the generators of a cone with vertex at the origin. The unrotated spheroidal coordinates (μ, θ) are related to the cartesian (ζ, r) by

$$\left.\begin{aligned} r &= \tfrac{\bar{\alpha}}{2} \cosh\mu \sin\theta \\ \zeta &= \tfrac{\bar{\alpha}}{2} \sinh\mu \cos\theta \end{aligned}\right\} \qquad (2.2)$$

Where $\bar{\alpha}$ is the interfocal distance common to the hyperbolas and ellipses. By eliminating μ the equation for the hyperbolas is

$$\left.\begin{aligned} \left(\frac{r}{\frac{\bar{\alpha}}{2}\sin\theta}\right)^2 - \left(\frac{\zeta}{\frac{\bar{\alpha}}{2}\cos\theta}\right)^2 &= 1 \\ \text{or} \qquad \left(\frac{r}{r_0}\right)^2 - \left(\frac{\zeta}{\zeta_0}\right)^2 &= 1 \end{aligned}\right\} \qquad (2.3)$$

By rotating the hyperbola specified by a given θ ($\bar{a}$ being fixed for the system) through $\varphi = 2\pi$, the hyperbolic horn is formed.

Expressing ψ as below, and putting in the wave equation (2.1),

$$\psi = M(\mu)\,\Theta(\theta)\,\phi(\varphi)\,e^{j\omega t}, \tag{2.4}$$

ϕ turns out to be given by

$$(d^2\phi/d\varphi^2) + a^2\phi = 0$$

Since ψ must return to the same value after φ goes through 2π, a must be an integer. The equation for the angular and radial functions are simplified if the following substitutions are made.

$$\left.\begin{aligned} \Theta &= W\cdot\sin^a\theta, \quad z = \cos\theta \\ M &= F\cdot\cosh^a\mu, \quad x = \sinh\mu \end{aligned}\right\} \tag{2.5}$$

Then

$$\left.\begin{aligned} (1-z^2)W'' - 2(a+1)zW' + (b-c^2z^2)W &= 0 \\ (1+x^2)F'' + 2(a+1)xF' - (b-c^2x^2)F &= 0 \end{aligned}\right\} \tag{2.6}$$

where

$$-c^2 \equiv (k\bar{\alpha}/2)^2 = (\bar{\alpha}\pi\nu/c_s)^2$$

and b is any of the characteristic values, to be determined by the boundary conditions.

The solution of the equation for the angular functions W was effected by noting that for $-c^2 = 0$, $W = P_n^m(Z)$, the associated legendre functions. The b's and W's may then be expanded in powers of $(-c^2)$ about $-c^2 = 0$, yielding nicely convergent series. It is found that the first few

W's show greatest dependency on frequency (in the $-c^2$ factor), and that the b's are nearly linear functions of $-c^2$. Freehafer's data is given in graph form for bounding hyperboloids specified by $\theta = 15°$ and $30°$; it is interesting to note that the W's for $-c^2 = 0$ are those for the conical horn of the same θ.

The radial functions presented more difficulty, for the equation for F has singular points at $\pm j$ and infinity; no contour was found which would give an integral representation. Recourse was had to the WKB method, which was found feasible for $-c^2$ not too near a value for which any b became zero. Since most of the low frequency energy is carried by the first term in the series expansion for ψ and the first characteristic value is zero for $-c^2 = 0$, the method is of doubtful application in this important case, where the low frequency behaviour is desired. Differential analyzer methods have been used for these F's, and when all the data is worked up, will present a practically complete picture.

The WKB method yields results as follows, with the above restriction on $-c^2$: there are two representations for F_n, one on each side of the point $x_n' = (b_n/c^2)^{\frac{1}{2}}$. Region I will include the space from $x = 0$ to $x = |x_n'|$ when $x_n' < 0$

and Region II the remainder. Then

$$\left.\begin{aligned} \text{I} \quad F_n &= \frac{e^{j\pi/4}}{\sqrt{2}} \frac{\exp\left[\int_x^{x_n'} \sqrt{\frac{|x_n'+x^2|}{1+x^2}}\,dx\right]}{\left[(|x_n'+x^2|)(1+x^2)\right]^{1/4}} \\ \text{II} \quad F_n &= \frac{\exp(-jk)\left[\int_{x_n'}^{x} \sqrt{\frac{x_n'+x^2}{1+x^2}}\,dx\right]}{\left[(x_n'+x^2)(1+x^2)\right]^{1/4}} \end{aligned}\right\} \qquad (2.7)$$

Note that in I the phase is constant at $\pi/4$ leading to an infinite phase velocity. This means that under such conditions the reaction of that particular elementary wave back on the piston is mainly that of the mass of air which moves as a unit. Also, when $x > |x_n'|$, the air behaves as a dispersive medium with phase velocity

$$w = \frac{c_s}{\sqrt{\frac{x_n'+x^2}{1+x^2}}} \qquad (2.8)$$

where c_s is the velocity from the wave equation. It should be noted, for reference in the next section, that if for the F equation of (2.6), we set

$$F_n = \frac{f_n}{\left[(x_n'+x^2)(1+x^2)\right]^{1/4}} \qquad (2.9)$$

then the equation for f_n is

$$f_n'' + f_n\left[-c^2\frac{x_n'+x^2}{1+x^2} - \frac{1}{(1+x^2)^2}\right] = 0 \qquad (2.10)$$

If rigid cisoidal piston motion with a velocity

$$\dot{\xi} = u_0 e^{j\omega t}$$

is assumed at the plane $\mu = 0$, the resulting velocity potential in the infinite horn is given by

$$\psi = u_0 e^{j\omega t} \sum \frac{\int_{z_0}^{1} W_n(z)\, dz}{\int_{z_0}^{1} W_n^2(z)\, dz} W_n(z) \frac{F_n(x)}{F_n'(0)} \qquad (2.11)$$

where $z_0 = \cos \theta_0$, the angle θ_0 being that determining the horn surface.

The above mathematical results may now be translated into the following qualitative predictions for the infinite hyperbolic horn:

1. The pressure amplitude field is simple at low frequencies and shows a fairly steady decrease outward along the axis. At higher frequencies this steady decrease is accompanied by periodic variations about the smoothed out steady decrease.

2. At low frequencies the phase of the pressure on the axis changes non-uniformly, but becomes more uniform as the frequency increases. At all frequencies the phase changes most slowly near the throat.

3. The variation of amplitude with angle increases with frequency, the most marked variation approaching the throat as the frequency increases.

4. The radiation resistance (as roughly computed by Freehafer and communicated privately to the author) should rise rapidly from zero as the frequency is increased until a peak about 36 % above the ultimate value is reached at $-c^2 = 1$. Then the resistance should fall asymptotically to the ultimate value.

In this section the mathematical results of the exact theory have been translated into terms of the quantities to be measured. Although applicable only to the infinite horn, the finiteness of the experimental system should not alter the type of result, but only the degree.

III PLANE WAVE ANALYSIS

The foregoing theory holds only for the infinite horn, which is difficult to simulate experimentally. In order to obtain a solution applicable to the actual horn it will be seen that the essential factor is the presence of the reflected wave. If we try to investigate the finite horn set in an infinite baffle, then the horn surface, including the baffle, is very different from that for the infinite horn. As the boundary value problem for surfaces other than those represented by setting one coordinate constant is still awaiting rigorous solution, we seek approximate methods. For the horn problem the usual approximation is to assume that plane waves in the horn represent a type of average behaviour which may be used to calculate the average performance. This analysis, first conceived by Webster[7], may be further extended in such a manner as to apply to any reasonably shaped horn. In what follows, then, we shall derive the wave equation for plane waves in a channel of changing section S, noting the necessary approximations, and obtain general results for the sound pressure and admittance at any section S, taking due account of the reflected wave. For comparison with previous results for conical and exponential horns, the solutions for these particular cases will be briefly indicated. The application to the hyperbolic horn will then

be discussed, and there will be given a general method of solution which will apply to any horn.

The wave equation will now be derived, using a Lagrangian procedure in which our attention is focussed on a given mass of the medium. Following Fig. 2,

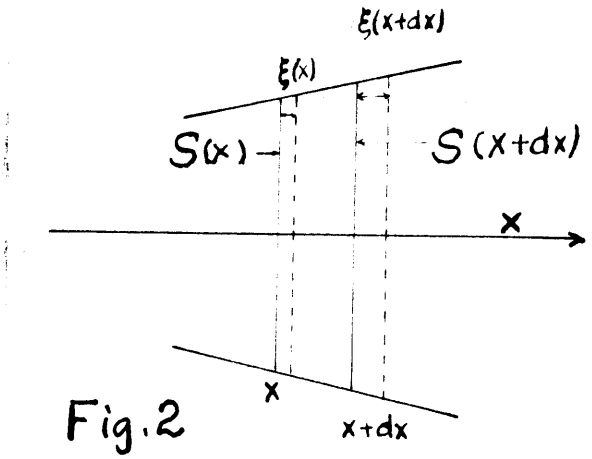

Fig. 2

we take this mass as the amount of air which when acoustically undisturbed is between the slab whose faces are fixed by the axial distances x and $x+dx$. ξ is the displacement as a function of x and t. $\bar{S}$ denotes the average area of the slab faces and for infinitesimal amplitudes is a function of x alone. By combining the equations of continuity, state and motion it is desired to express the sound pressure p as a function of x, t and S.

Continuity conditions are satisfied by demanding that the mass of air remain unchanged, or that the product

$$\rho_0 S dx$$

remain constant. Then under disturbed conditions the mass is

$$\rho\, \bar{S}(x+\xi) \cdot \left[dx + \frac{\partial \xi}{\partial x} dx \right]$$

which when we assume that ξ is very small, becomes

$$\rho\, dx \left(\bar{S} + \xi \frac{\partial \bar{S}}{\partial x}\right)\left(1 + \frac{\partial \xi}{\partial x}\right)$$

$$\simeq \rho\, dx \left(\bar{S} + \bar{S} \frac{\partial \xi}{\partial x} + \xi \frac{\partial \bar{S}}{\partial x}\right)$$

or

$$\rho_0\, dx\, \bar{S} \simeq \rho\, dx \left(\bar{S} + \frac{\partial (S\xi)}{\partial x}\right) \qquad (3.1)$$

where the product $\xi \frac{\partial \bar{S}}{\partial x} \frac{\partial \xi}{\partial x}$ has been neglected on the assumption that not only ξ but also $\partial \bar{S}/\partial x$ is small. We note that S is also a function of ξ because in the Lagrangian procedure it is the face of a particular mass of air; but with infinitesimal ξ, S is substantially a function of x alone, as it rigorously would be in an Eulerian treatment. Practically this means that the horn must not flare too rapidly, and that the intensity of the sound must be such as to keep ξ small at least where $\partial S/\partial x$ is large.

Returning to (3.1), we set

$$\frac{\rho - \rho_0}{\rho} = -\frac{1}{S} \frac{\partial (S\xi)}{\partial x} = \frac{\delta \rho}{\rho}$$

in which we use S for $\bar{S}$, subject to the above restrictions. In the last member of this equation we note the infinitesimal $\delta\rho/\rho$; for use in the wave equation this may be approximated by $\delta\rho/\rho_0$, since $\delta\rho \ll \rho$.

Hence the equation of continuity is

$$\frac{\delta \rho}{\rho_0} = -\frac{1}{S}\frac{\partial(S\xi)}{\partial x} \tag{3.2}$$

To replace density by pressure, it has been generally assumed and amply demonstrated that the adiabatic law is followed at least for all intensities of sound below that causing pain. Thus

$$P\,V^{\gamma} = \text{constant}$$

or

$$\frac{\delta P}{P} = -\gamma\frac{\delta V}{V} \tag{3.3}$$

for small changes in pressure and volume, which holds under the conditions indicated above. Since the mass is constant in our Lagrangian treatment, $V \propto 1/\rho$, (3.3) becomes

$$\frac{\delta P}{P_0} = -\gamma\frac{\delta V}{V_0} = \gamma\frac{\delta \rho}{\rho_0} \approx -\frac{1}{S}\frac{\partial(S\xi)}{\partial x} \tag{3.4}$$

Since δP is the sound pressure p, we set finally

$$p = -\gamma P_0 \frac{1}{S}\frac{\partial(S\xi)}{\partial x} \tag{3.5}$$

In order to introduce time, the force equation is applied to the faces of the slab. Taking forces to the right as positive, and assuming $p << P_0$, the equation of motion is

$$\bar{S}\left[\left(P_0 + p + \frac{\partial p}{\partial x}dx\right) - (P_0 + p)\right] = \frac{\partial}{\partial t}\left[\rho_0 \bar{S}dx\,\frac{\partial(x+\xi)}{\partial t}\right]$$

where $x + \xi$ denotes the instantaneous position of the

slab. Simplifying,

$$\frac{\partial^2 \xi}{\partial t^2} = -\frac{1}{\rho_0}\frac{\partial p}{\partial x} \qquad (3.6)$$

The wave equation for p may now be obtained by eliminating ξ from (3.5) and (3.6). Form

$$\frac{\partial^2 p}{\partial t^2} = -\frac{\gamma P_0}{S}\frac{\partial^2}{\partial t^2}\left[\frac{\partial}{\partial x}(S\xi)\right]$$

$$= -\frac{\gamma P_0}{S}\frac{\partial}{\partial x}\left[\frac{\partial^2}{\partial t^2}(S\xi)\right]$$

Since under the assumptions mentioned in connection with the continuity equation S is a function of x alone,

$$\frac{\partial^2 p}{\partial t^2} = -\frac{\gamma P_0}{S}\frac{\partial}{\partial x}\left(S\frac{\partial^2 \xi}{\partial t^2}\right)$$

$$= \frac{\gamma P_0}{\rho_0}\frac{1}{S}\left(S\frac{\partial p}{\partial x}\right)$$

$$\text{or} \quad \frac{1}{S}\frac{\partial}{\partial x}\left(S\frac{\partial p}{\partial x}\right) - \frac{1}{c^2}\frac{\partial^2 p}{\partial t^2} = 0 \qquad (3.7)$$

Equation (3.7) is substantially that derived by Webster, and applied to specific horns by later workers. The main assumptions (other than the plane wave picture) may be summarized by stating that the amplitudes of the field quantities p and ξ must be small, and that S must not change too quickly with x, or at least not where ξ is large, as at the throat.

With cisoidal time variation of $e^{j\omega t}$ (3.7) becomes

$$\frac{1}{S}\frac{d}{dx}\left(S\frac{dp}{dx}\right) + k^2 p = 0 \qquad (3.8)$$

For checking with experiment, p should be regarded as an average value over each section. Since in a plane wave (in which the velocity is approximately in phase with the pressure) the intensity varies with p^2 (8), the average pressure should best be represented by

$$\bar{p} = \sqrt{\frac{\int_S \int p^2 dS}{S}} \qquad (3.9)$$

taken over each section S. However, at low frequencies for which the actual wave fronts approach the plane wave condition, the values on the axis are sufficient.

Returning to a general solution for (3.8), a hint as to the possible form for p is obtained from the physics of the situation. Using the intensity variation with p as above, then the product

$$p^2 S = P_A$$

must be constant in a progressive wave for which p is uniform over S, in order to keep constant the power P_A transmitted. Thus the variation of p as a function of x will be due, to a great extent, to a factor

$$\frac{1}{\sqrt{S}}$$

Hence by setting

$$p = \frac{f}{\sqrt{S}} \tag{3.10}$$

the function f will be given the task of representing the variations of p about the steady decrease of $1/\sqrt{S}$.

The mathematical arguments for this form for p are still simpler. Equation (3.8) is of the self adjoint type, for which the substitution of (3.10) yields an equation for f of the form

$$f'' + Bf = 0, \quad B = B(S,x), \tag{3.11}$$

the first derivative being lacking. The advantage of (3.11) is that many of the numerical methods of integration now used in atomic physics may be directly applied, yielding results for most cases of interest.

However, before finding the form of B(S,x), we pause to change to non-dimensional variables, leaving physical constants to fix the dimensions of the final solutions. First, from the equation for the horn profile we seek a unit of length so that x may be expressed as a ratio. In general this is possible, as seen from the relations below for conical, exponential and hyperbolic horns.

$$\begin{aligned} &\text{Conical horn} && r = r_0 (x/x_0) \\ &\text{Exponential horn} && r = r_0 e^{(x/x_0)} \\ &\text{Hyperbolic horn} && r = r_0 \sqrt{1+(x/x_0)^2} \end{aligned} \tag{3.12}$$

Hence we set

$$\alpha \equiv \frac{x}{x_0} \tag{3.13}$$

The section $S = \pi r^2$ becomes $S = S_0 \gamma$, where:

$$\begin{aligned} &\text{Conical horn} && \gamma = \alpha^2 \\ &\text{Exponential horn} && \gamma = e^{2\alpha} \\ &\text{Hyperbolic horn} && \gamma = 1+\alpha^2 \end{aligned} \tag{3.14}$$

$$S_0 = \pi r_0^2$$

If we finally define

$$\beta = k x_0 \; ; \qquad k = \frac{2\pi\nu}{c} \tag{3.15}$$

and express the wave equation (3.8) in terms of α, β and γ, we get

$$\frac{1}{\gamma}\frac{d}{d\alpha}\left(\gamma \frac{dp}{d\alpha}\right) + \beta^2 p = 0 \tag{3.16}$$

and substituting

$$p = \frac{f}{\sqrt{\gamma}}$$

the equation for f turns out to be

$$f'' + \left[\beta^2 + \left(\frac{\gamma'}{2\gamma}\right)^2 - \left(\frac{\gamma''}{2\gamma}\right)\right] f = 0 \tag{3.17}$$

where the primes refer to differentiation by α.

Before going on to a general solution for p, we give briefly the form for f when the γ for conical and exponential horns is inserted, in order to note the agreement with the results of previous and different modes of attack [9,10].

Conical horn;

$$\left.\begin{aligned} &\gamma = \alpha^2 \\ &f'' + \left[\beta^2 + \left(\tfrac{1}{\alpha}\right)^2 - \tfrac{1}{\alpha^2}\right] f \simeq f'' + \beta^2 f = 0 \\ &f = e^{\mp j\beta x} = e^{\mp jkx} \\ &\quad = \cos\beta x \mp j \sin\beta x \\ &\quad = \cos kx \mp j \sin kx \end{aligned}\right\} \quad (3.18)$$

where the upper sign is for the outgoing wave.

Exponential horn;

$$\left.\begin{aligned} &\gamma = e^{2\alpha} \\ &f'' + \left[\beta^2 + 1 - 2\right] f = f'' + (\beta^2 - 1) f = 0 \\ &f = e^{\mp j\alpha\sqrt{\beta^2-1}} = e^{\mp jkx\sqrt{1-\left(\frac{1}{kx_0}\right)^2}} \\ &\quad = \cos\sqrt{\beta^2-1}\,\alpha \mp j \sin\sqrt{\beta^2-1}\,\alpha \\ &\quad = \cos kx\sqrt{1-\left(\tfrac{1}{kx_0}\right)^2} \mp j \sin kx\sqrt{1-\left(\tfrac{1}{kx_0}\right)^2} \end{aligned}\right\} \quad (3.19)$$

In this last case the cut-off at $\beta = 1$ is clearly apparent.

Using the value of γ for the hyperbolic horn, the equation for f turns out to be

$$f'' + \left[\beta^2 + \left(\frac{\alpha}{1+\alpha^2}\right)^2 - \frac{1}{1+\alpha^2}\right] f$$
$$= f'' + \left[\beta^2 - \frac{1}{(1+\alpha^2)^2}\right] f = 0$$

This is very nearly the same as the equation for f_1 of the set (2.10), for b_1/c^2 is close to unity when the

angular opening of the horn is small. Thus at low frequencies the plane wave picture is essentially the same as that from exact theory.

Returning now to the general solution, we first assume that f may be expressed as

$$f = g e^{\mp jh} \tag{3.20}$$

or

$$f = u \mp jv \tag{3.21}$$

where in general, g and h or u and v are functions of α. We relate the first and second forms for f in the simplest manner, namely

$$u = g \cos h$$
$$v = g \sin h$$

Thus, the first form represents a sinusoidal variation of varying amplitude. This representation is advantageous for most horns, for at large values of α most horns give an equation for f of the type

$$f'' + B_o f = 0,$$

where B_o is constant. Under these conditions, the first form represents f most directly. The second form has its greatest utility in the numerical integration sometimes necessary to obtain f, for here both u and v satisfy the equation for f.

It is desired to obtain a general expression for the pressure and admittance, the latter being defined as

$$Y = \frac{\dot{\xi}}{p}$$

It will prove easier to obtain the latter quantity first. From equation (1.2)

$$Y = \frac{-\nabla \psi}{\rho_0 (\partial \psi / \partial t)} \tag{3.22}$$

and with cisoidal time variation and plane waves

$$Y = -\frac{(d\psi/dx)}{j k \rho_0 c \psi}$$

Setting

$$y \equiv Y \rho_0 c \tag{3.23}$$

we get

$$y = -\frac{(d\psi/dx)}{j k \psi}$$

By some simple juggling it is easily shown that p and ψ obey the same wave equation; hence

$$y = -\frac{(dp/dx)}{j k p}$$

or in terms of non-dimensional variables

$$y = \frac{1}{\beta} \cdot \frac{p'}{p} \; ; \; \beta = k x_0 \; ; \; \alpha = \frac{x}{x_0} \tag{3.24}$$

where the primes refer to differentiation with respect to α. Substitution from (3.16) and (3.21) gives

$$y_{\pm} = \frac{1}{\beta} \left[\frac{u' \mp j v'}{u \mp j v} - \frac{\gamma'}{2\gamma} \right] \tag{3.25}$$

Rationalizing,

$$y_{\pm} = \pm \frac{1}{\beta} \left(\frac{uv' - vu'}{u^2 + v^2} \right) - \frac{1}{\beta} \left(\frac{\gamma'}{2\gamma} - \frac{uu' + vv'}{u^2 + v^2} \right) \tag{3.26}$$

where the upper of the double signs is for the outgoing wave. Note that the negative real part of y- corresponds to energy returning to the source in the reflected wave. Thus, the signs for the total pressure and velocity are contained in y, so that

$$\left.\begin{aligned} p &= p_+ + p_- \\ \dot{\xi} &= \dot{\xi}_+ + \dot{\xi}_- = y_+ p_+ + y_- p_- \end{aligned}\right\} \qquad (3.27)$$

In order to obtain y, some sort of relation must be assumed between p_+ and p_-. In general, these quantities may differ only in amplitude and phase; and since we are interested in the variation of p and y with distance, it is advantageous to state this relation in a form for which the distance factor is confined to one term. This is done by setting

$$\left.\begin{aligned} p_\pm &= g\, e^{\mp j h} \cdot e^{\pm(\psi_0 + j\varphi_0)} \\ \frac{p_+}{p_-} &= e^{2\psi_0 + j2(\varphi_0 - h)} \end{aligned}\right\} \qquad (3.28)$$

where the ψ_0 and φ_0 are the arbitrary amplitude and phase constants, usually to be determined by conditions at the mouth of the horn.

Using the form $f = g\, e^{\mp j h}$, and proceding as before,

$$y_\pm = \pm \frac{1}{\beta} - \frac{1}{\beta}\left(\frac{r'}{2r} - \frac{g'}{g}\right) \qquad (3.29)$$

Then y in terms of the total pressure and velocity gives

an expression reducing to

$$\left.\begin{aligned} y &= \frac{h'}{\beta}\tanh\left[\psi_0 + j(\varphi_0 - h)\right] - \frac{1}{\beta}\left(\frac{\gamma'}{2\gamma} - \frac{g'}{g}\right) \\ \text{or}\quad y &= \frac{1}{\beta}\cdot\frac{uv' - vu'}{u^2+v^2}\tanh\left[\psi_0 + j\left(\varphi_0 - \tan^{-1}\frac{v}{u}\right)\right] \\ &\quad - \frac{1}{\beta}\left(\frac{\gamma'}{2\gamma} - \frac{uu'+vv'}{u^2+v^2}\right) \end{aligned}\right\} \qquad (3.30)$$

Likewise, the total pressure turns out to be

$$\left.\begin{aligned} p &= p_+ + p_- \\ &= \sqrt{\frac{u^2+v^2}{\gamma}}\cosh\left[\psi_0 + j(\varphi_0 - \tan^{-1}\tfrac{v}{u})\right] \\ &\equiv P\, e^{-j\theta} \\ P &= \sqrt{\frac{u^2+v^2}{\gamma}\left[\cosh^2\psi_0 - \sin^2(\varphi_0 - \tan^{-1}\tfrac{v}{u})\right]} \\ \theta &= -\tan^{-1}\left[\tanh\psi_0\tan(\varphi_0 - \tan^{-1}\tfrac{v}{u})\right] \end{aligned}\right\} \qquad (3.31)$$

These results may be directly applied to any reasonably shaped horn when the function f has been evaluated, numerically or otherwise. For checking with the previous conical and exponential horn results[9], the form $f = g\,e^{\mp jh}$ is best; but for calculation, the form $f = u \mp jv$ is necessary, as both u and v satisfy the

equation for f. The method of calculating f is described in Appendix A, and the results for four values of the frequency parameter β are listed as Appendix B.

The constants ψ_0 and φ_0 may be obtained in two ways: by mouth impedance, and by the pressure along the axis. In the first case, if the mouth is provided with an infinite baffle, the admittance y is converted to its reciprocal (the impedance $z = Z/\rho_0 c$) and compared at the mouth with that obtained by assuming the vibrating at the mouth replaced by an ideal piston, the impedance of which is given by Plate 1. The constants ψ_0 and φ_0 may then be evaluated analytically, but graphical means using a chart plotting the conversion

$$r + jx = \tanh(\psi + j\varphi)$$

is preferable. If the mouth has no baffle, the mouth impedance may be approximated by methods described by Crandall[11] or McLachlan[12].

When the pressure along the axis is known, the constants may be determined from the equation for P in (3.31), by requiring that the theoretical curve fit the experimental one in amplitude (for ψ_0) and position along the axis (for φ_0).

To summarize the results of this section, we have used Webster's assumption of plane waves for the starting point of an analysis applicable to any horn whose section

does not change too violently with position. The generalized results agree with those for the conical and exponential horns as obtained by previous procedures. As a direct application, some f functions have been computed for the hyperbolic horn, and are listed in an Appendix, together with the general method of solution.

IV EXPERIMENTAL TECHNIQUE

The general experimental work may be divided into two parts, the first dealing with the amplitude and phase of the sound field, and the second with the impedance at the throat. In each there was used a horn of $\theta_o = 15°$, or of 30° total angular opening.

For the field measurements, it was desired to have the throat large enough to enable a Hall type minimic to be inserted in to at least 10 cm from the piston without distorting the sound field too much. It was found that if the interfocal distance (Freehafer's $\bar{a}$) of 30 cm were used, then the ratio of microphone area to throat area would be less than 1/10. Also, at the highest frequency at which stable measurements were possible (2000 hz), the microphone was less than $\lambda/10$ in overall dimensions, so that little reflection was expected. With these constants θ_o and $\bar{a}$, the resulting hyperbola is

$$\left(\frac{r}{3.88}\right)^2 - \left(\frac{\zeta}{14.49}\right)^2 = 1$$

For $\zeta > 50$ cm, it was found that a cone of half angle 14° 50' would fit closely enough from there on, so the mouth section was made in this shape from #18 guage galvanized iron. For the throat part a wooden pattern, accurately turned to the desired profile, was obtained and used as the core in a cement casting together with a joining collar. On removal of the core the surface was finished

Electromagnetic Driver
Longitudinal Section

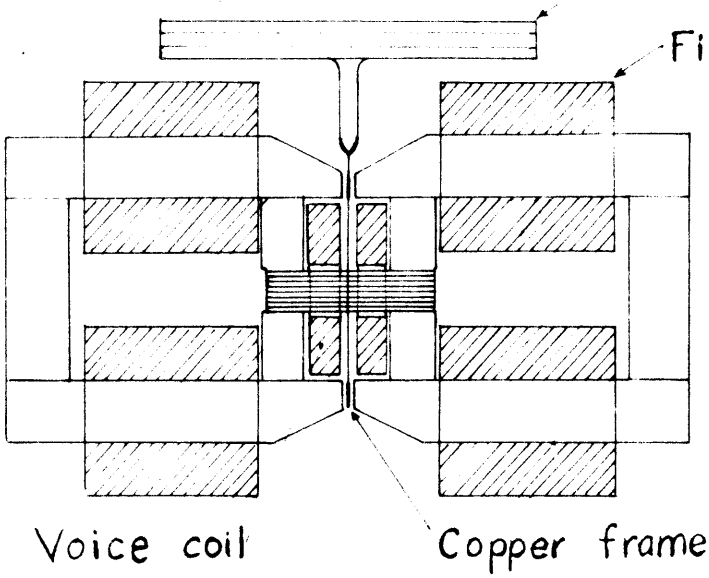

Frame Support
Top

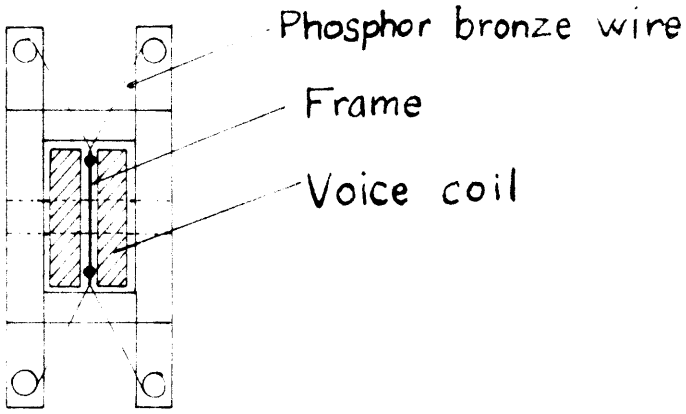

Plate 2

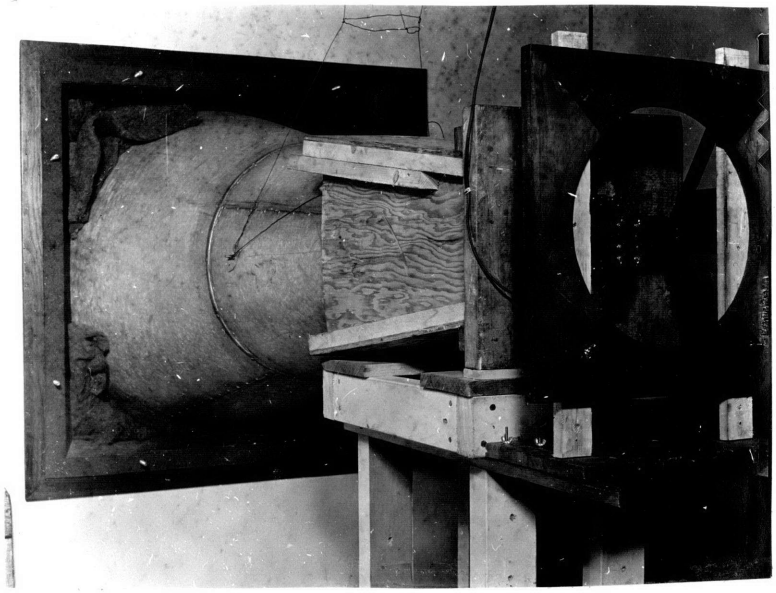

Source Room

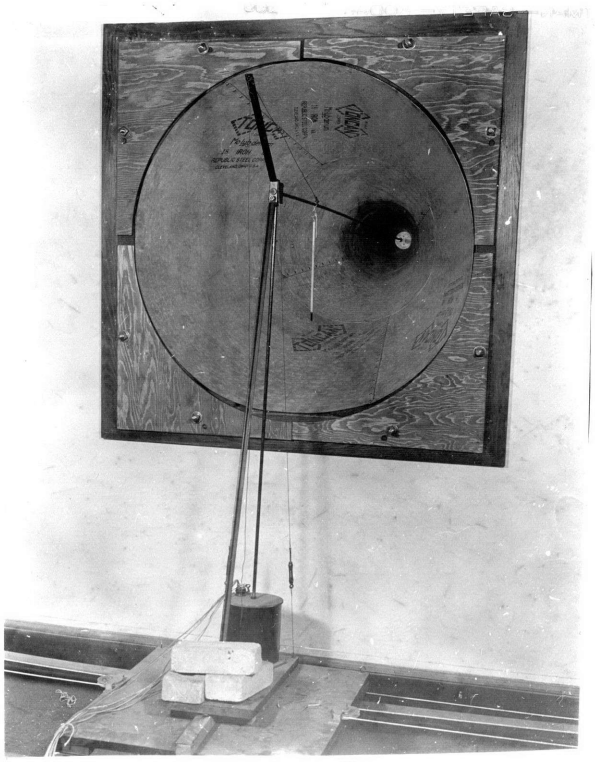

Measuring Room

Plate 3

with paraffin to the dimensions and smoothness desired; and by the joining collar the mouth and throat pieces were fastened together to form a horn of 7.76 cm throat diameter, 96.8 cm mouth diameter, and 180 cm long.

For a driving unit there was used a mechanism invented by Prof. Fay at M.I.T., as shown in plate 2. Briefly, it is a transformer whose secondary, a flat rectangular copper frame, is made to move in its own plane by the interaction of the current induced in it by the primary, and a steady magnetic field. Phosphor bronze wires serve to constrain the motion along one direction, and may be used to tune the unit to resonance by adjusting the tension. As a piston there was used three layers of 4mm balsa wood, cemented together with the grain crossed. Chladni figure tests showed that rigid piston motion obtained for frequencies well above the highest used in the experiment. No impedance measurements were made on the unit, for due to the iron and air losses involved, and the permanently closed circuit of the copper frame, not all the parameters could be obtained.

The horn and driver were suitably mounted together, and the horn placed with its mouth firing through the one bare wall of the otherwise well-damped booth in the Electrical Engineering Dept. Sound Lab. See Plate 3. The Hall type minimic was mounted on a platform whose position could be set from the outside to about $\pm$ 0.8 cm from its original position, after having been displaced in two dimensions.

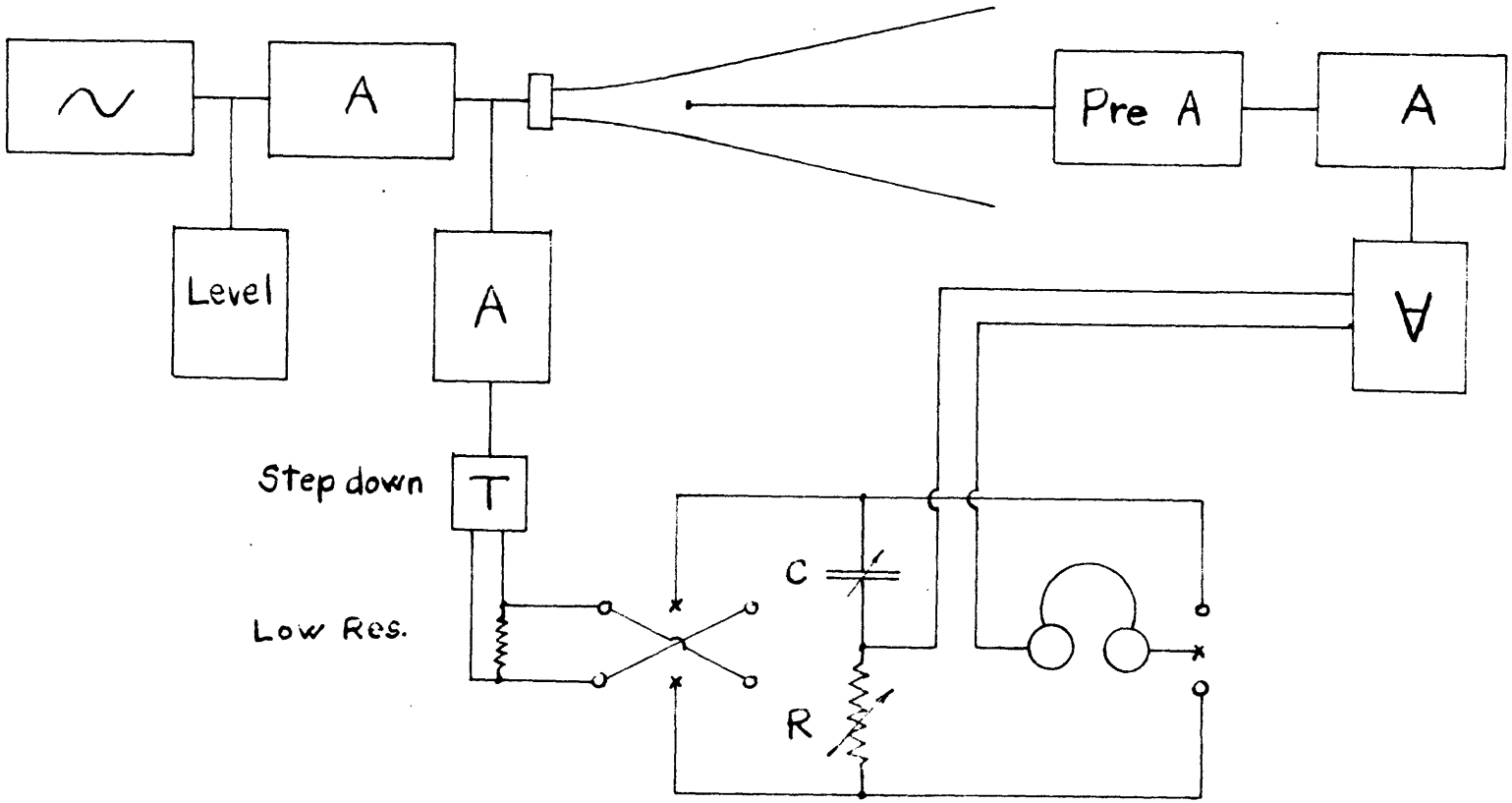

Plate 4

Measurement of Pressure Amplitude and Phase

Practically, this means that if the pressure shows fairly sharp peaks, occurring every $\lambda/2$, then noticeable difficulty in setting and checking will come around 2500 hz, where this uncertainty as to setting will distort the pressure curve, because $\frac{1}{4}\frac{\lambda}{2} \simeq 1.6$cm at this frequency. Most of the difficulty was in the lack of smooth motion, causing the microphone lead pipe to swing to a new stable position.

Plate 4 indicates the circuit used for determining the relative amplitudes and phases by means of comparing the output of the microphone with a portion of the input to the driving unit. It was assumed that the phase relations in the amplifiers were not functions of amplitude over the range used. This was checked by varying the input to the driver, and changing the attenuator $\forall$ ("nay") to restore balance as indicated by the phones. With the two to three figure accuracy obtainable at most balance settings, this effect was negligible.

Data was obtained in the form of contours of equal amplitude and phase, which are presented and discussed in the next section. Runs on the axis were also taken to provide data as free as possible from shifts in the field structure due to slight temperature or frequency changes.

For all the field measurements the plane 10 cm from the piston was chosen as the fiducial point, the amplitude 100 and the phase zero being arbitrarily assigned there. Field plots in rather large detail were obtained for the

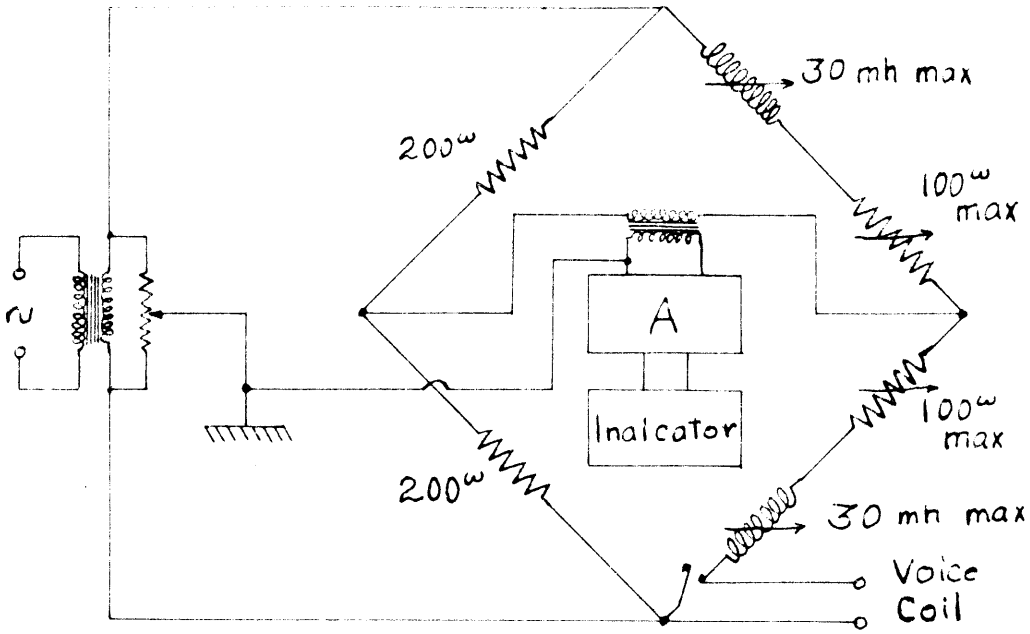

Measurement of Receiver Impedance

Substitution Method

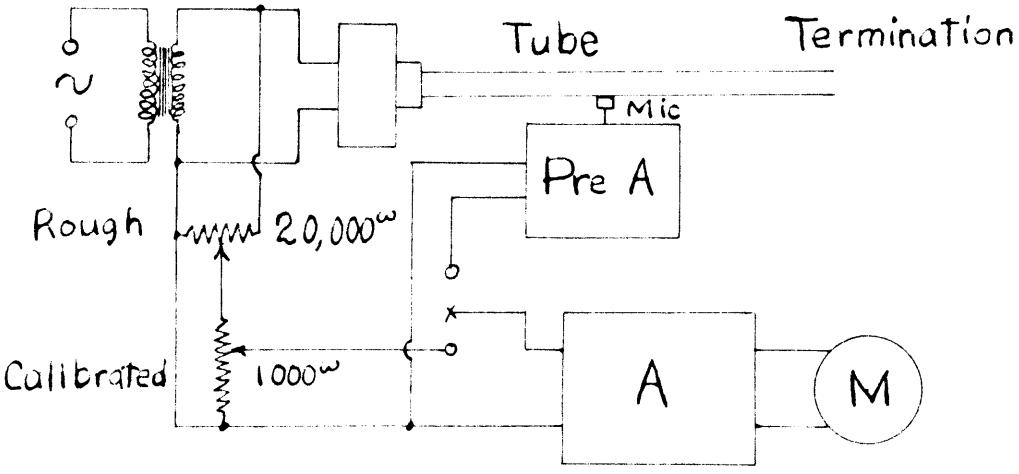

Acoustic Line Circuit

Output Compared with Input

Plate 5

first 130 cm of the 180 cm horn, while runs on the axis were extended to 170 cm from the piston, the limit of the microphone travel. The frequency parameter of the exact theory, $-c^2$, was used with values of .2 5, .5, 1, 2, 8 and 30 corresponding roughly to frequencies of 180, 250, 360, 510, 1000 and 2000 hz respectively. Since in $-c^2$ it is $k\frac{\alpha}{2}$ which must be constant, the frequency had to be adjusted with temperature, as the value of the wave velocity varies with temperature. Results were nicely reproducible as to all essential features except for the highest value of $-c^2$, at 2000 hz. Here the run had to be gone through rapidly after the salient features had been picked out, as the field was unstable and the settings critical.

Impedance tests were made on another 15° horn of the same conical mouth, but provided with a throat piece going to 3/4" diameter at the driver fitting. The equation of the hyperbola was

$$\left(\frac{r}{95}\right)^2 - \left(\frac{\xi}{3.56}\right)^2 = 1$$

and it was found that the total length came out to be 182 cm, using the same mouth diameter as before.

The driving unit was the Western Electric Type 555 telephone receiver; and by using a modification (suggested by Fay) of the Fay-Hall impedance circle method[13], input impedance measurements on the receiver were used to obtain the air load on the receiver, and hence the throat impedance.

By this measurements down to 120 hz were possible, although difficult; a substitution bridge as shown in Plate 5 was set up, and phones, copper oxide meter and tuned vibration galvanometer used as null indicators. Incidentally the use of the meter indicator turned out to be the best technique all around, for whenever the balance was broad, a setting at the average of settings a given amount off balance was always possible.

For the lowest frequencies, this meter method was the only one available, and was applied up to 400 hz. However, above 300 hz the acoustic line described by Fay and Hall at the November 1938 Acoustical Society meeting was more convenient and accurate, and so was applied up to 4000 hz. Above this the readings became too irregular to interpret safely, but the interesting portion of the impedance was well within this range.

V RESULTS AND DISCUSSION

The experimental results fall into two groups: the data from pressure measurements, and that from impedance measurements. For both cases graphical presentation is used; and whenever possible calculations from theory is also shown on the graph. In general, the results are relative, not absolute, and non-dimensional variables are used throughout.

Field Measurements

In Plates 6, 7 and 8 are shown the contours of constant phase and pressure obtained by the circuit of Plate 4. Frequency is stated in terms of the parameter

$$-C^2 = \left(\frac{\pi \nu \alpha}{C_s}\right)^2 \cong \left(\frac{\nu}{360}\right)^2$$

the latter value being for the horn investigated. Each plate depicts the field at two frequencies, as the symmetry was sufficient to justify giving but half. The lower frequency is at the right. At the fiducial point 10 cm from the piston the amplitude 100 and phase zero were arbitrarily assigned, all other values being relative to these.

Turning now to the low frequency fields mapped on Plate 6, we recall the predictions of the exact theory (page 13). First, the amplitude and phase contours are nearly coincidental for $-c^2 = .25$, for which $\nu \simeq 180$ hz. Along the axis the pressure decreases steadily with but

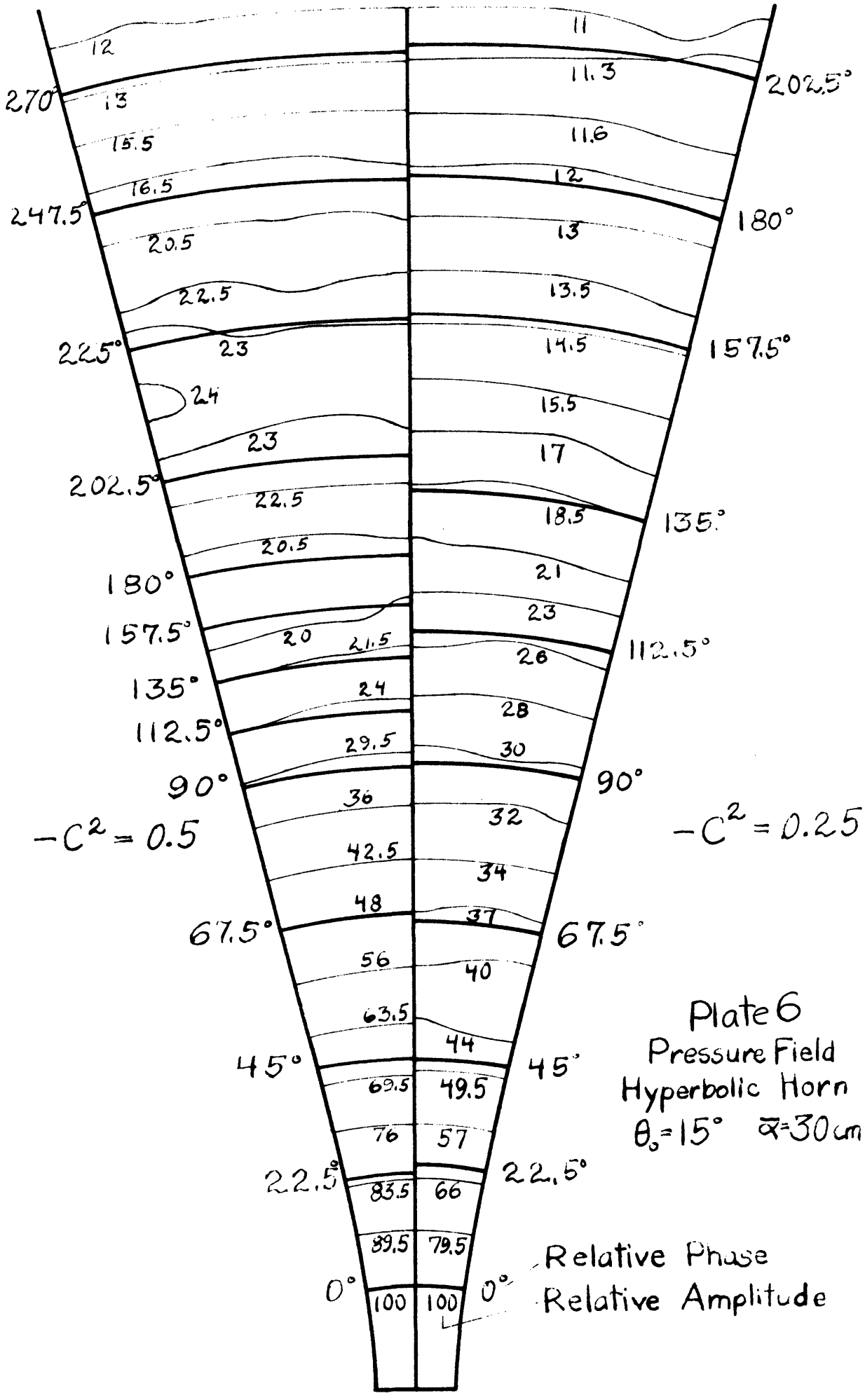
270°
247.5°
225°
202.5°
180°
157.5°
135°
112.5°
90°
67.5°
45°
22.5°
0°
202.5°
180°
157.5°
135°
112.5°
90°
67.5°
45°
22.5°
0°
12
13
15.5
16.5
20.5
22.5
23
24
23
22.5
20.5
20
21.5
24
29.5
36
42.5
48
56
63.5
69.5
76
83.5
89.5
100
11
11.3
11.6
12
13
13.5
14.5
15.5
17
18.5
21
23
26
28
30
32
34
37
40
44
49.5
57
66
79.5
100
$-C^2 = 0.5$
$-C^2 = 0.25$
Plate 6
Pressure Field
Hyperbolic Horn
$\theta_0 = 15°$ $a = 30$ cm
Relative Phase
Relative Amplitude

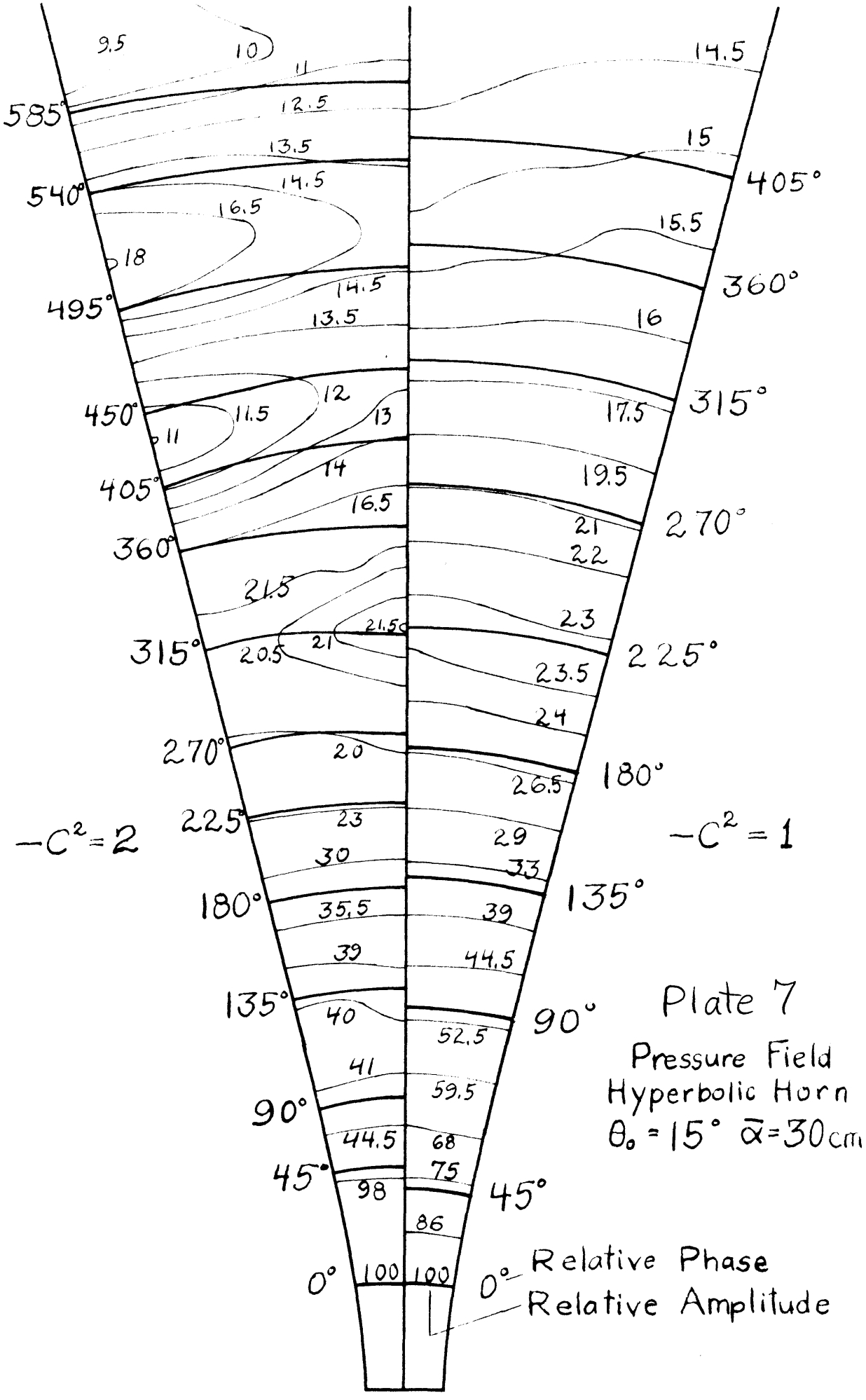
9.5
10
11
12.5
13.5
14.5
16.5
18
14.5
13.5
12
11.5
11
13
14
16.5
21.5
21
21.5
20.5
20
23
30
35.5
39
40
41
44.5
98
100
14.5
15
15.5
16
17.5
19.5
21
22
23
23.5
24
26.5
29
33
39
44.5
52.5
59.5
68
75
86
100
585°
540°
495°
450°
405°
360°
315°
270°
225°
180°
135°
90°
45°
0°
405°
360°
315°
270°
225°
180°
135°
90°
45°
0°
$-C^2=2$
$-C^2=1$
Plate 7
Pressure Field
Hyperbolic Horn
$\theta_0 = 15°$ $\bar{\alpha} = 30$ cm
Relative Phase
Relative Amplitude

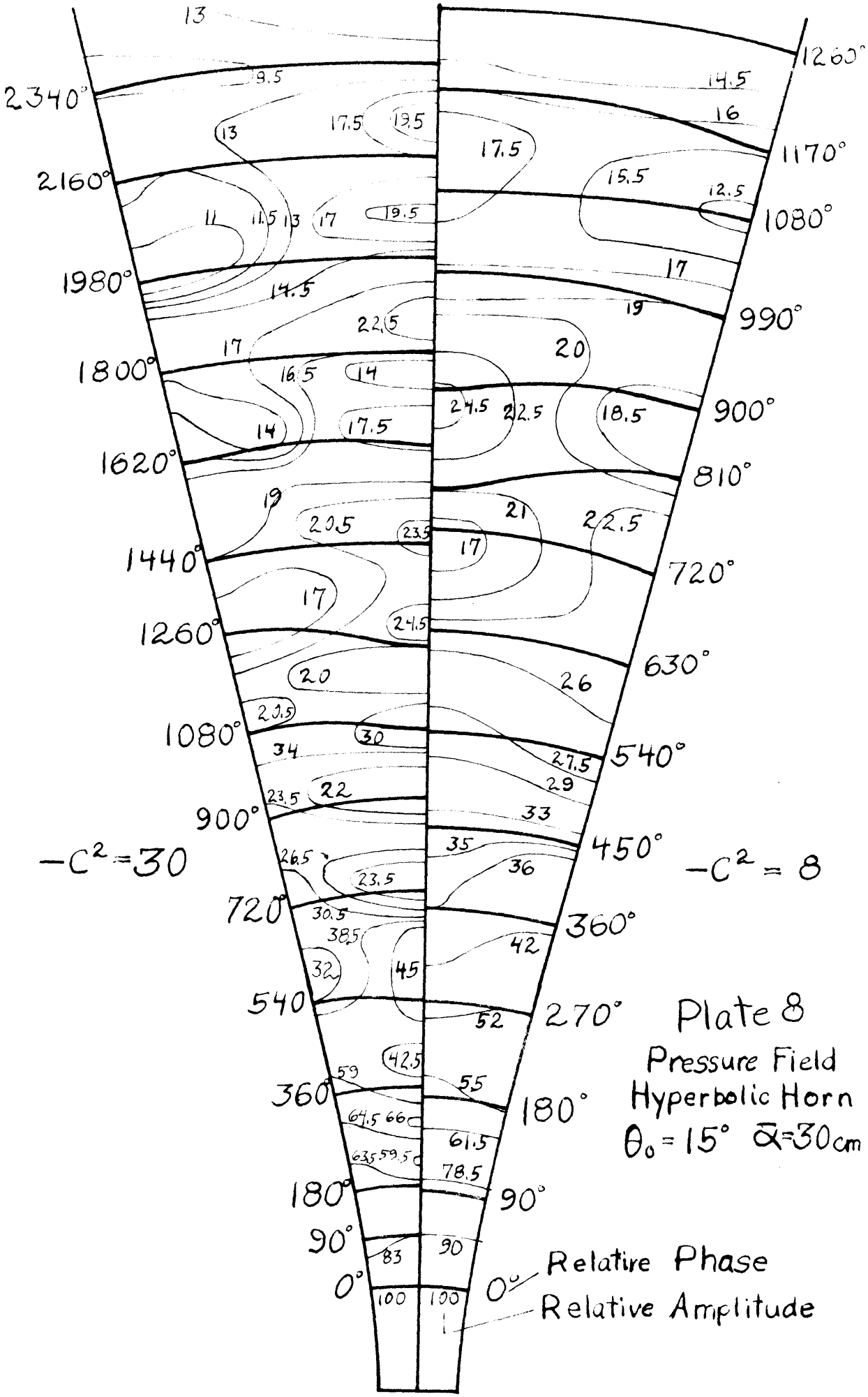
2340°
2160°
1980°
1800°
1620°
1440°
1260°
1080°
900°
720°
540°
360°
180°
90°
0°
1260°
1170°
1080°
990°
900°
810°
720°
630°
540°
450°
360°
270°
180°
90°
0°
$-C^2=30$
$-C^2=8$
Plate 8
Pressure Field
Hyperbolic Horn
$\theta_0=15°$ $\alpha=30cm$
Relative Phase
Relative Amplitude

small variations about the smoothed out decrease. The phase advances uniformly, and the contours in the mouth portion are practically those for a spherical wave. There is only slight variation with angle from the axis.

For $-c^2 = .5$ ($\nu \simeq 250$ hz) slightly more complexity is evident, mostly in the amplitude field which now shows definite variation with angle and the beginning of isolated regions of pressure extremes. The change of phase is markedly irregular at the center of the plot. This is not predicted by the infinite horn theory, but may safely be attributed to the presence of the reflected wave, due to the finite length of the horn. The approximate plane wave analysis has been applied to calculate this variation, the results of which will be discussed in connexion with Plates 9 and 10.

The middle frequency conditions of Plate 7 show the increased dependence on angle in the $-c^2 = 2$ ($\nu \simeq 500$ hz) plot. Since the particle velocity lies along the pressure gradient, the presence of transverse vibrations is apparent at the regions of maxima and minima at the horn surface. Here the picture is definitely changed by the presence of reflections, for in the third pressure "island" from the throat, the amplitude shows a definite increase with angle, which should not take place so markedly otherwise. The lack of information as to the value of the derivative of the radial functions (F_n) at the throat precludes an

exact evaluation, but since the room is certainly reflecting appreciably from the walls at this frequency, the incoming wave is not inconsiderable.

The other field on Plate 7, for $-c^2 = 1$ ($\nu \simeq 360$) shows substantially the same behaviour as the low frequency plots of Plate 8, and so needs no further discussion. However, the irregularity in spacing of the phase contours is now greatest near the throat, showing the influence of the rapid change of section there; the relatively smooth change farther along the axis is not a safe hint as to the magnitude of the reflected wave. Although the effect on the phase may be small, the effect on the amplitude may be quite large, as the other plots indicate.

At the highest frequencies chosen, corresponding to $-c^2 = 8$ ($\nu \simeq 1000$ hz) and $-c^2 = 30$ ($\nu \simeq 2000$ hz), the fields as given by Plate 8 show how the amplitude contours may become very complicated, while the equal-phase contours remain simple and uniformly spaced. The amplitude islands along the axis come at approximately the positions predicted by the exact theory, as verified by a rough calculation using but one term of the expansion for the velocity potention (Eq. 2.11). However, the values do not fluctuate (about the smoothed decrease along the axis) as much as the infinite horn theory predicts, indicating that the terminating conditions are still not able to simulate the infinite horn.

Next, in order to find how well the approximate plane wave theory corresponded to the measurements, the amplitude and phase of the pressure on the axis was measured, the plots for which are Plates 9 to 14 inclusive. As before, 10 cm from the throat has been taken as the fiducial point; but the amplitude has been multiplied by the factor $\sqrt{1+\alpha^2}$ which represents the smoothed out decrease. In symbols,

$$p\sqrt{\gamma} = p\sqrt{1+\alpha^2} = f$$

where f represents the oscillatory part of p.

The value at the fiducial point of a hundred arbitrary units, and at the first maximum, were fitted to the theoretical value

$$\sqrt{1+\alpha^2}\,p = \sqrt{u^2+v^2}\,\cosh\left[\psi_0 + j\left(\varphi_0 - \tan^{-1}\frac{v}{u}\right)\right]$$

$$= \sqrt{(u^2+v^2)\left[\cosh^2\psi_0 - \sin^2\left(\varphi_0 - \tan^{-1}\frac{v}{u}\right)\right]}$$

$$\times e^{j\tan^{-1}\left[\tanh\psi_0 \tan\left(\varphi_0 - \tan^{-1}\frac{v}{u}\right)\right]}$$

in order to determine the constants ψ_0 and φ_0. Then these same constants were used in the calculation of the phase, affording a fairly independent check. Because of the irregularities in the modified amplitude plot, fits were attempted only for values of the frequency parameter $\beta^2 = k\zeta_0)^2 \simeq \left(\frac{\nu}{380}\right)^2$ of .255 and .466, or frequencies of about 180 and 250 hz.

Plates 9 and 10 present the results of both experiment and the above plane wave calculation for the values

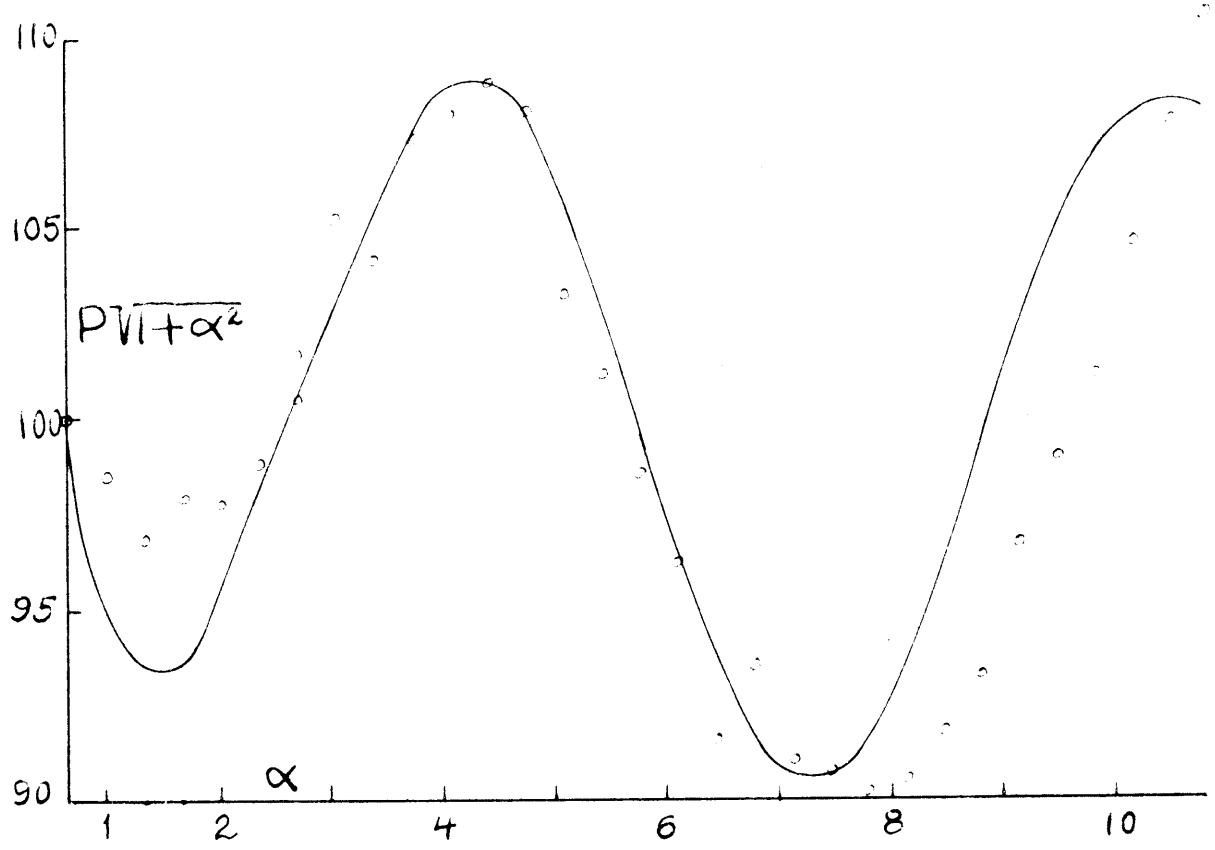

Pressure on Axis $Pe^{-j\theta}$

$\beta^2 = .255$

——— Theory

o o o Exp.

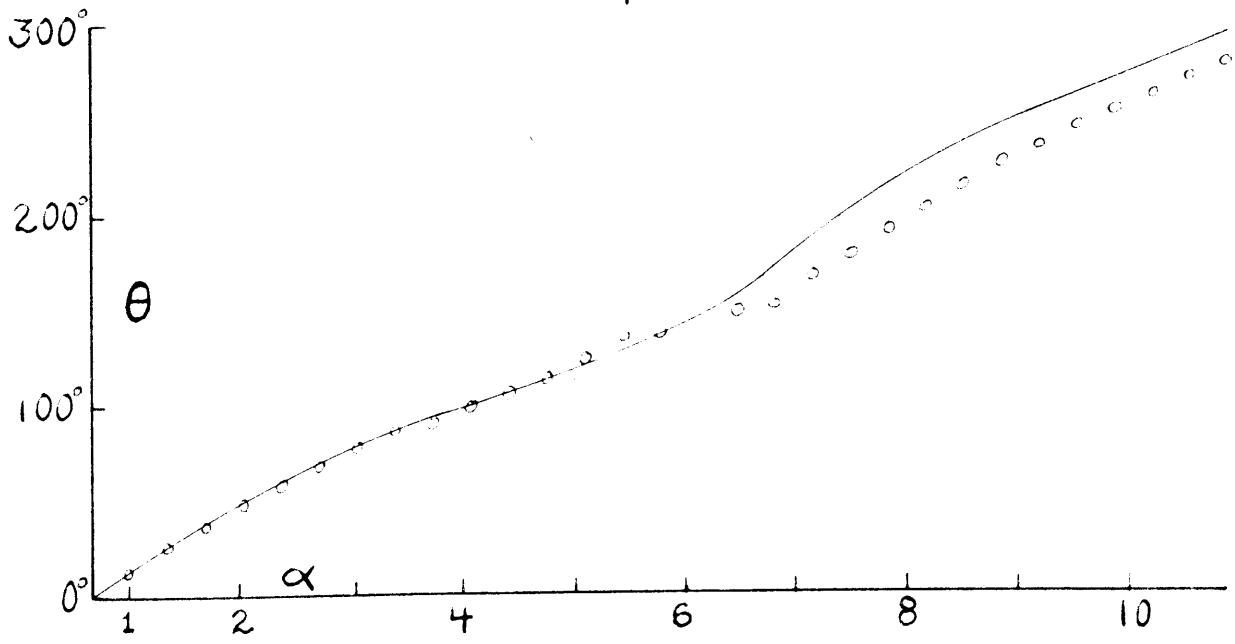

Plate 9

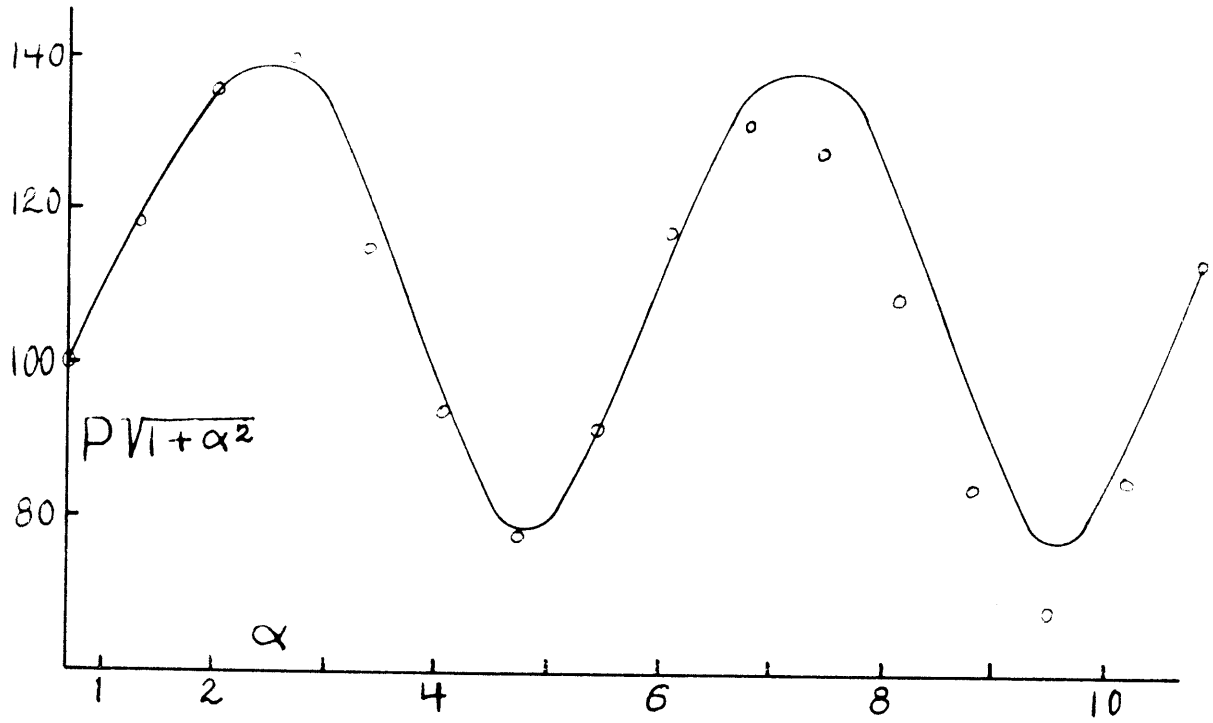

Pressure on Axis $Pe^{-j\theta}$

$\beta^2 = .466$

— Theory

° ° Exp.

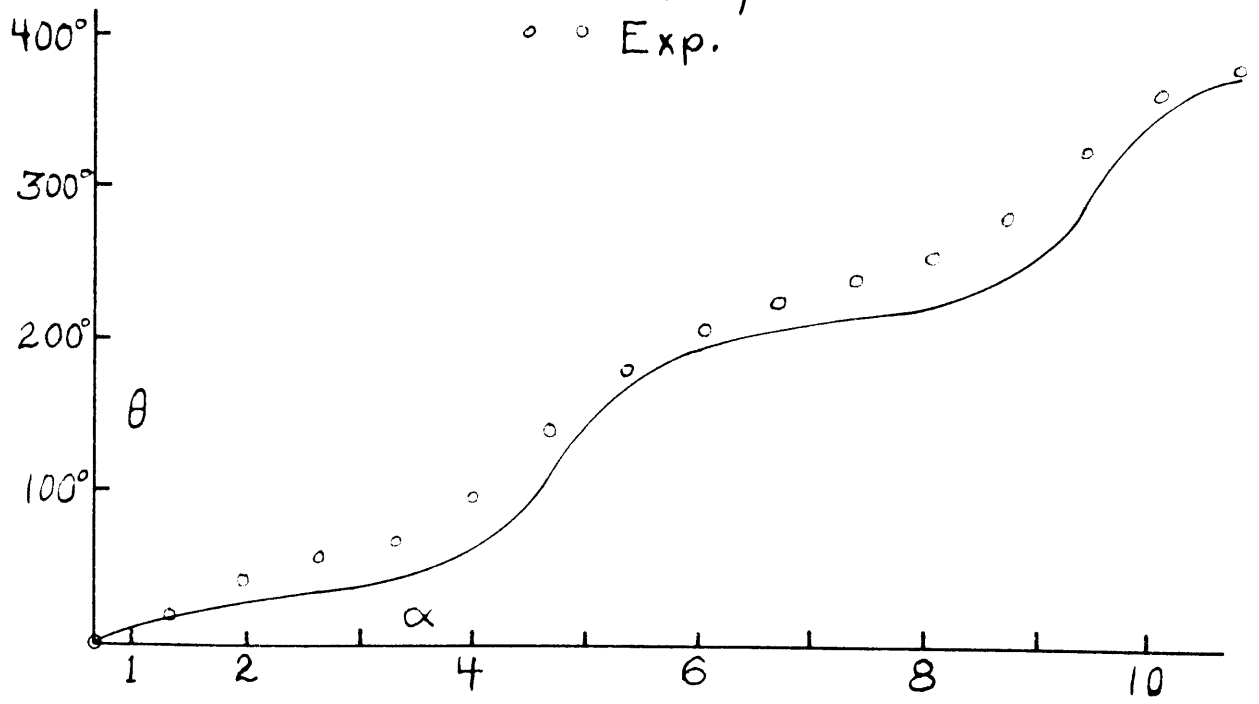

Plate 10

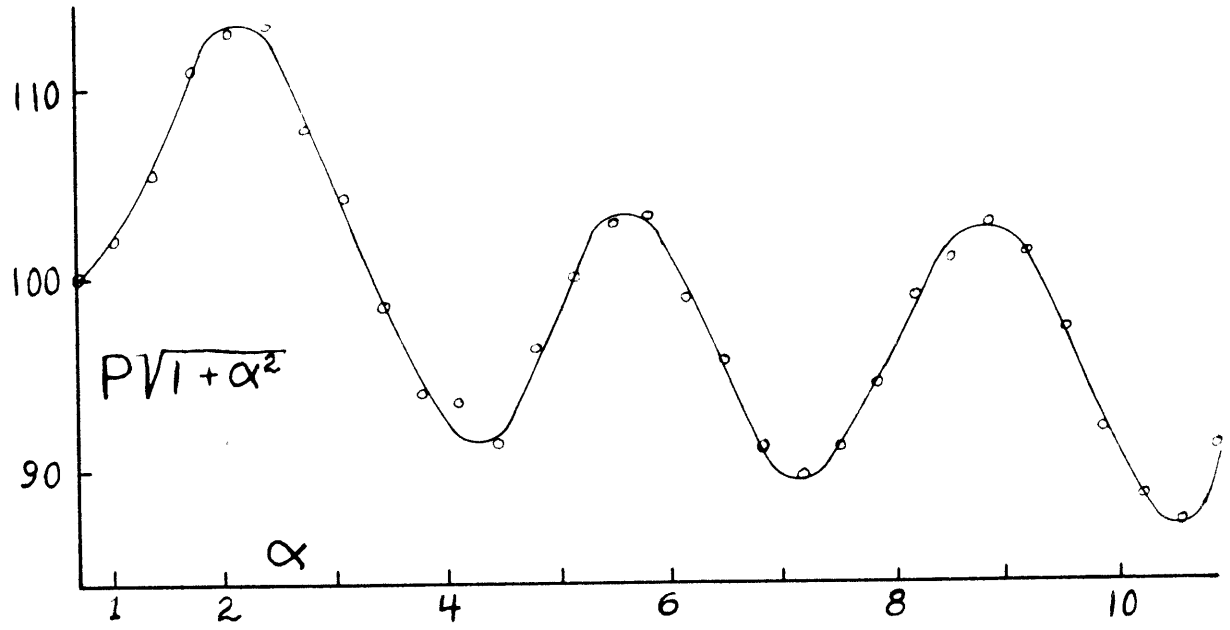

Pressure on Axis $Pe^{-j\theta}$

$\beta^2 = .933$

Exp. only

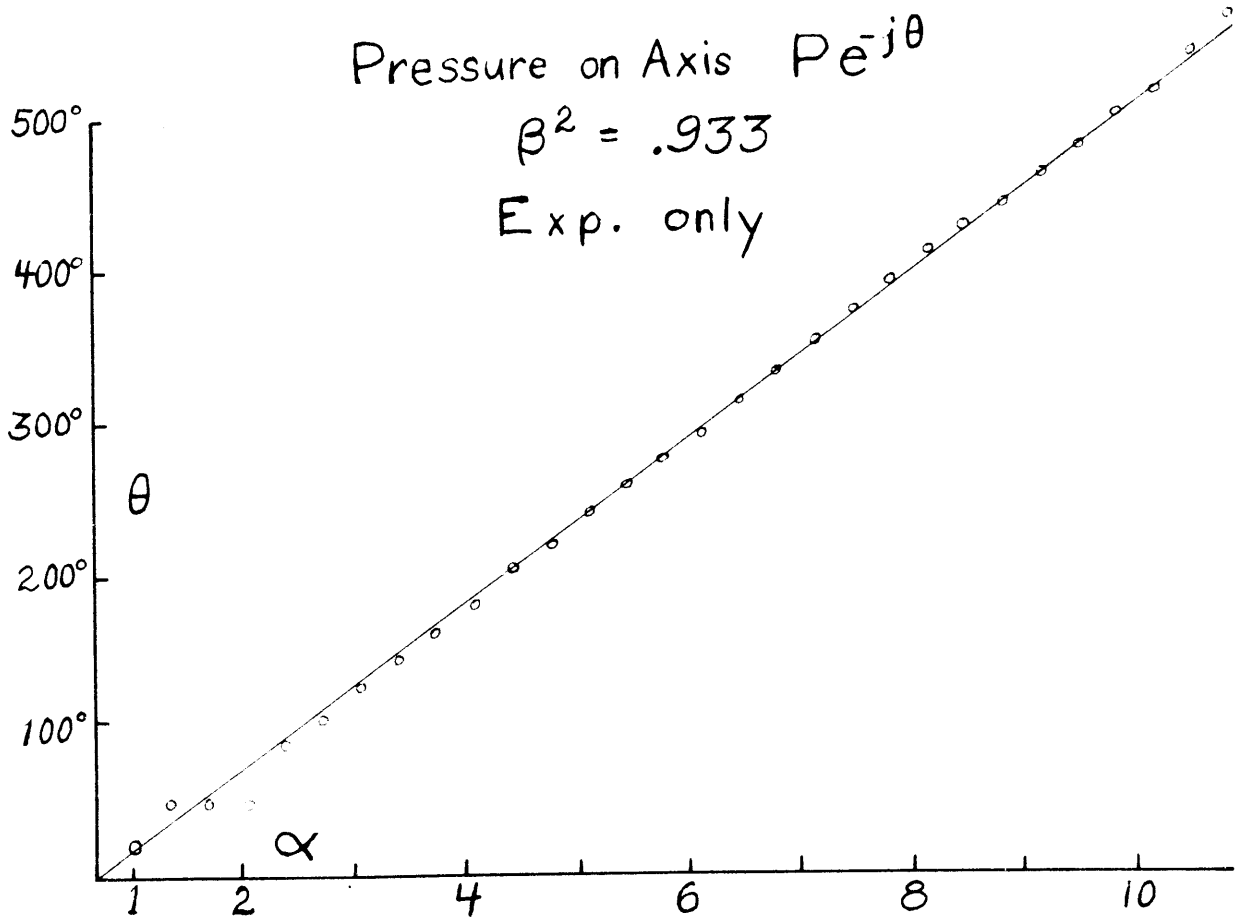

Plate II

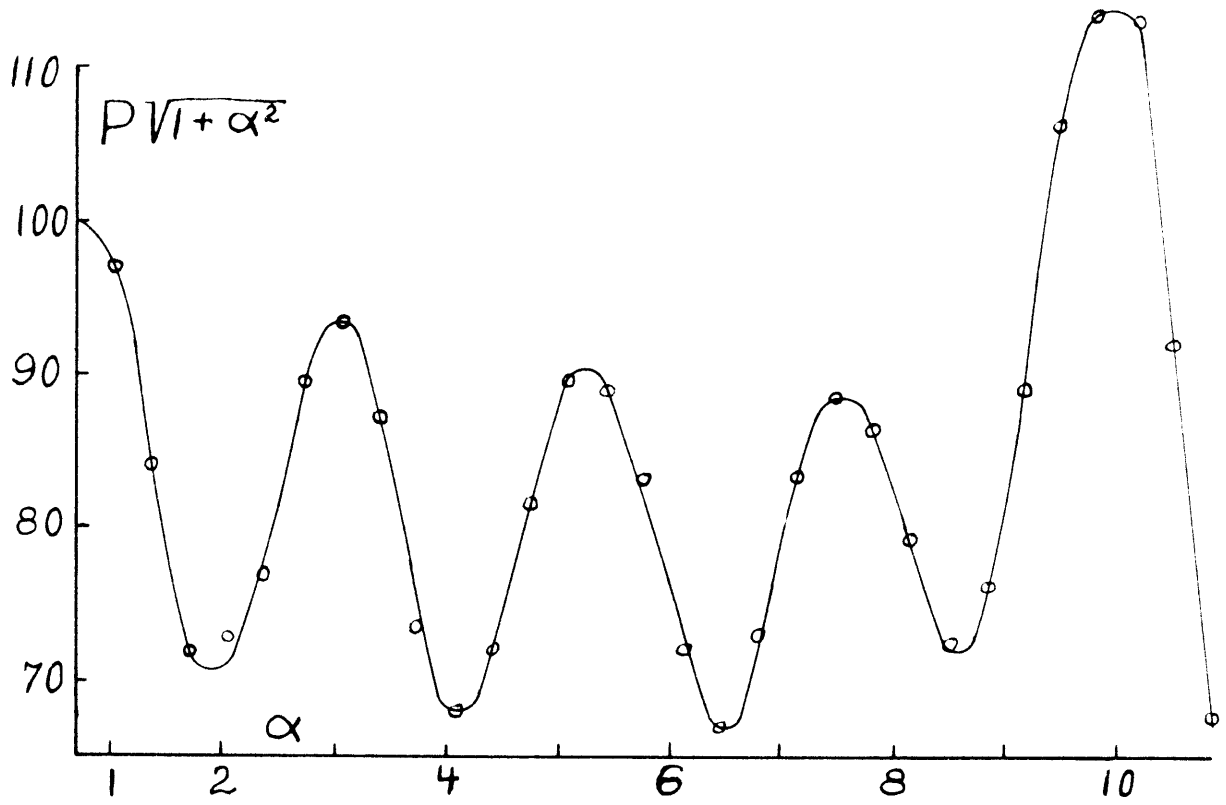

Pressure on Axis $Pe^{-j\theta}$

$\beta^2 = 1.87$

Exp. only

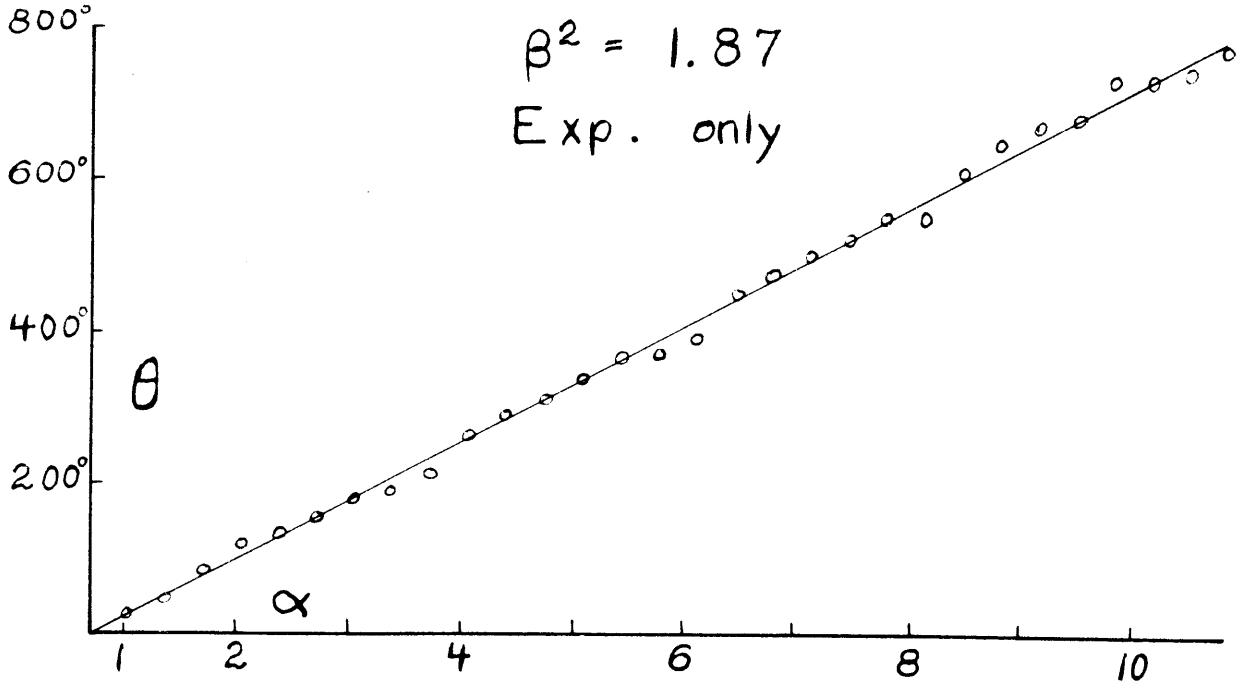

Plate 12

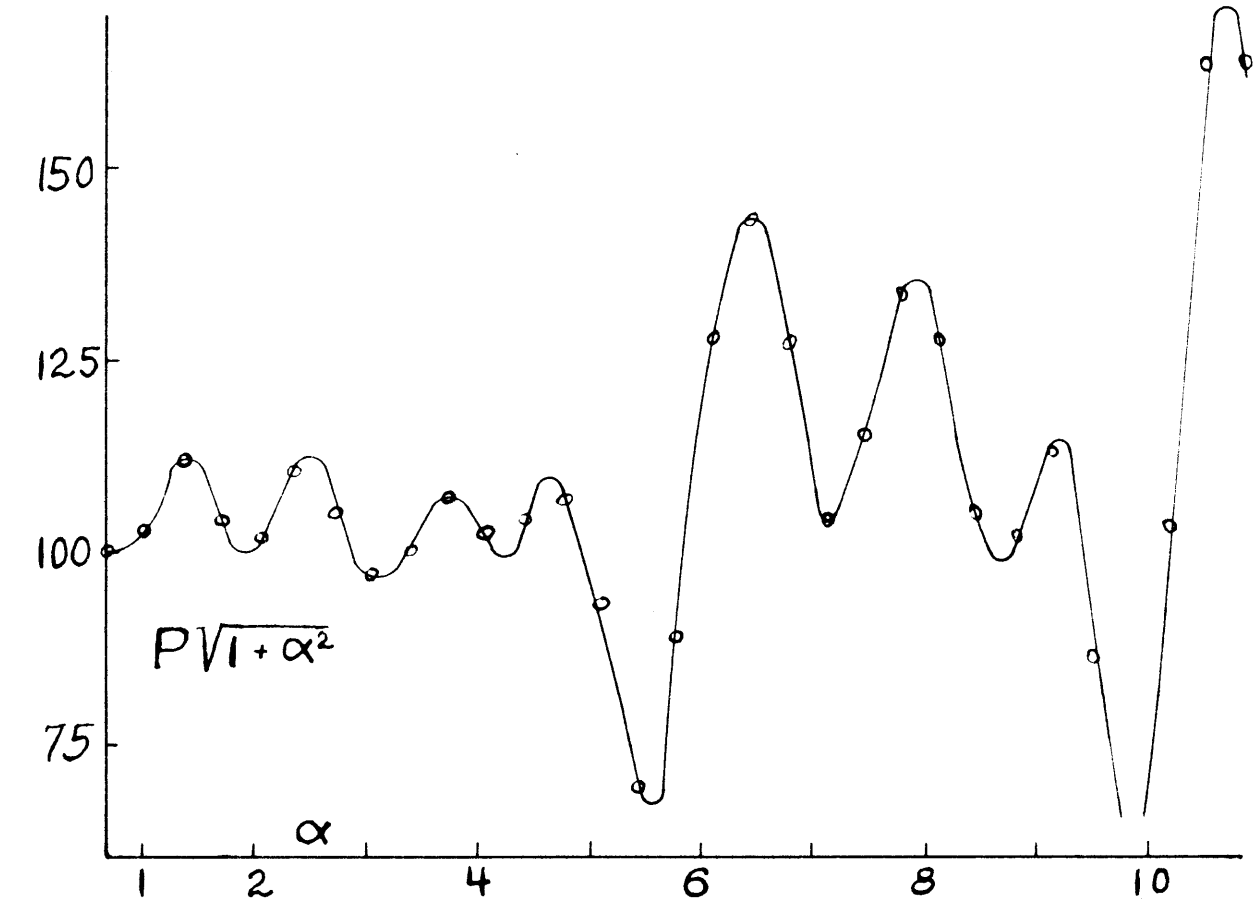

Pressure on Axis $Pe^{-j\theta}$

$\beta^2 = 7.46$

Exp. only

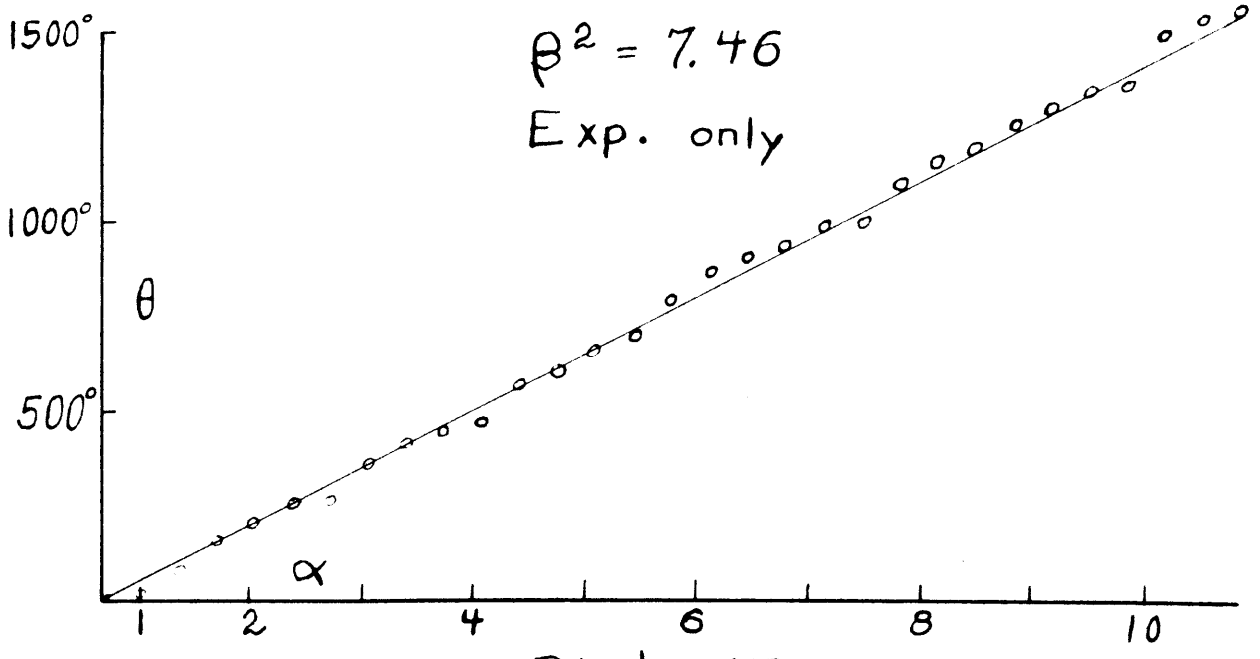

Plate 13

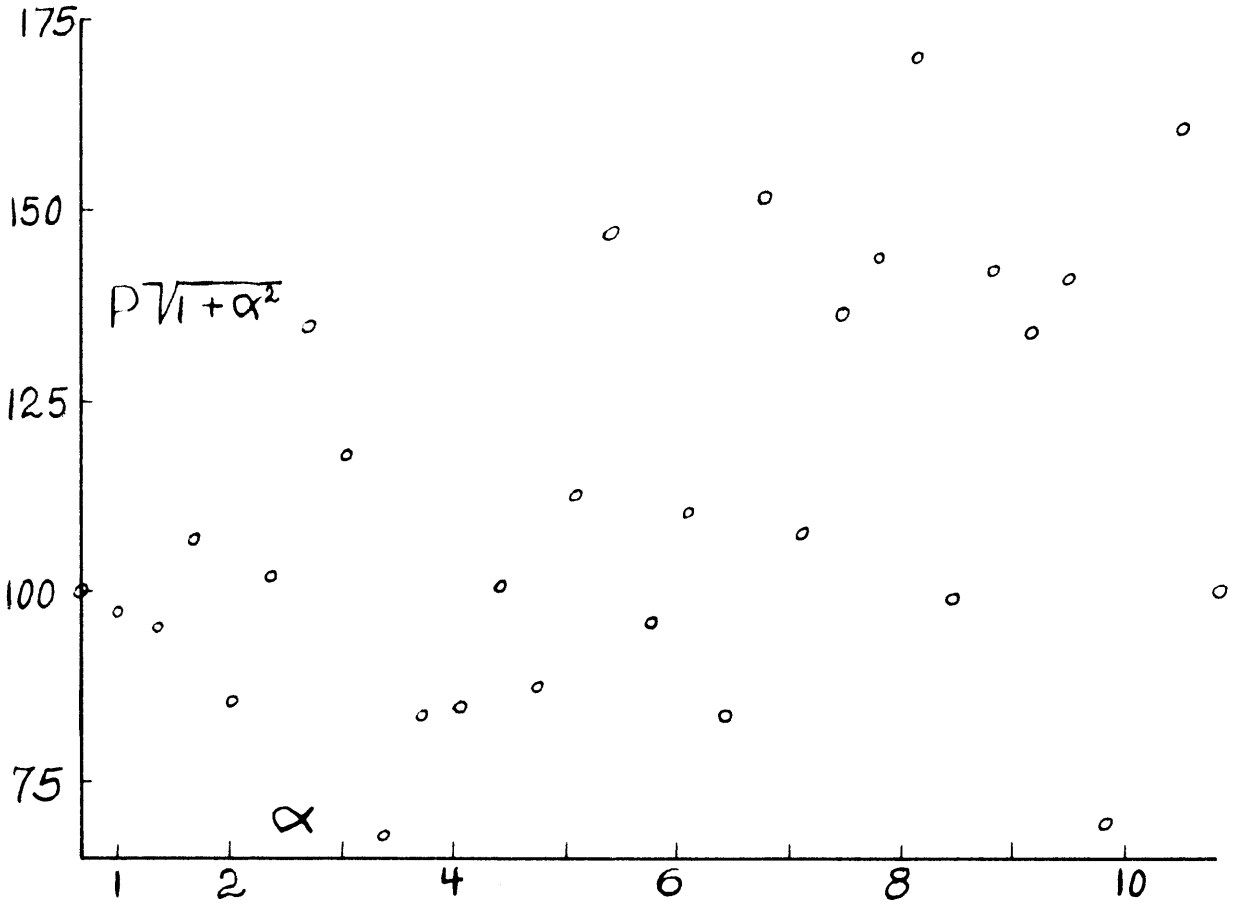

Pressure on Axis $Pe^{-j\theta}$

$\beta^2 = 28.0$

Exp. only

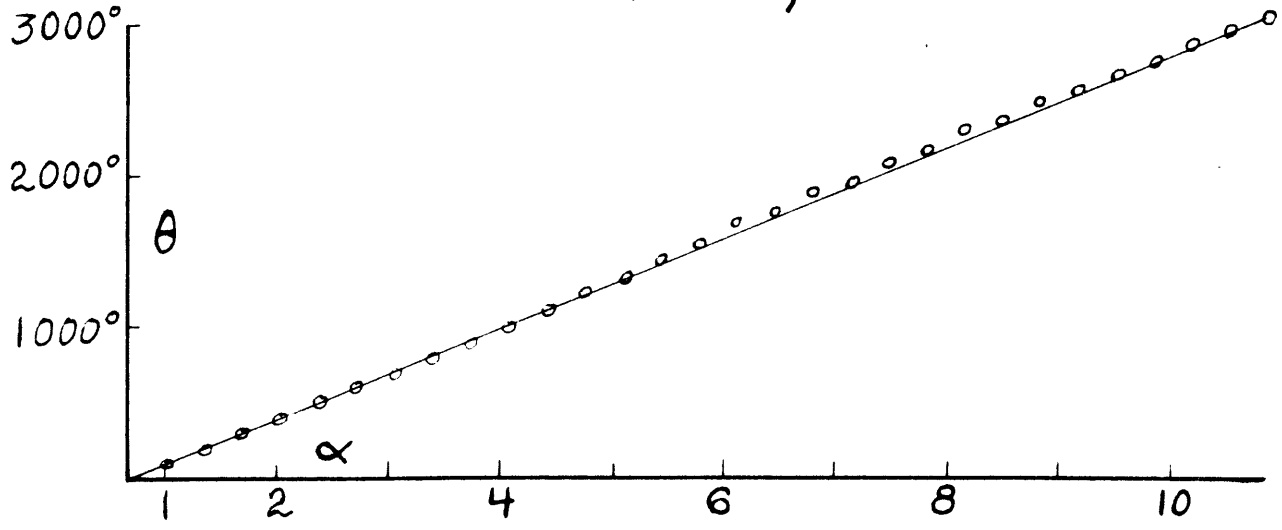

Plate 14

of β^2 mentioned. Although the fit is only approximate, it agrees with the field plots of Plate 6 in showing the assumption of plane waves to be a good one for these frequencies. The irregularities in the purely experimental amplitude plots for the higher frequencies of Plates 11, 12, 13 and 14 show that although the phase surfaces of the field plots suggest plane wave fronts, the variation of amplitude over the wave front is considerable; as again checked by referring to the field plots. More regularity would be expected if the values to be checked had been experimentally averaged over each cross section, as suggested by equation (3.9).

The last four plates mentioned also show the increasing regularity in the change of phase, for which the best curve becomes a straight line at large β^2. Thus the phase velocity, which is proportional to the reciprocal of the slope, shows less variation as the frequency increases, and approaches the wave velocity eventually.

For Plate 14, the points on the amplitude plot have not been connected, for the experimental points were not taken close enough together to resolve the rapid oscillations. However, it is noted that the amplitude of variation is greatest here, showing that the conditions of the exact theory are being approached.

To sum up, the pressure measurements show general agreement with the exact and plane wave analyses, when the

finiteness of the horn and termination is given due consideration. The plane wave picture is particularly applicable at low frequencies, providing some means of evaluating the two arbitrary constants ψ_0 and φ_0 is possible.

Impedance Measurements.

The two experimental techniques mentioned earlier gave overlapping results which agreed nicely in spite of their sensitivity to inequalities in temperature, etc. The measured resistance and reactance components are presented in the non-dimensional form $Z/S_0\rho_0 c$. Plate 15 uses the frequency parameter β as the abscissa, while Plate 16 compares the smoothed results with those for the idealized conical horn by impedance loci.

To consider first the behaviour with frequency, we first note that the abscissa for Plate 15 is $\beta \sim \nu/1540$, for the horn described in Section IV. This high value of ν_0 allows measurements to be easily made in the range most interesting in the theory, for the experimental technique is difficult at extreme frequencies.

The curves have been smoothed, for the resonances due to the finiteness of the horn occur less than 100 hz apart, and as the points attained are not close enough, connecting them would give a false picture. However, the general predictions of the exact theory are verified in the upper curve for the resistance, which exhibits the rise to

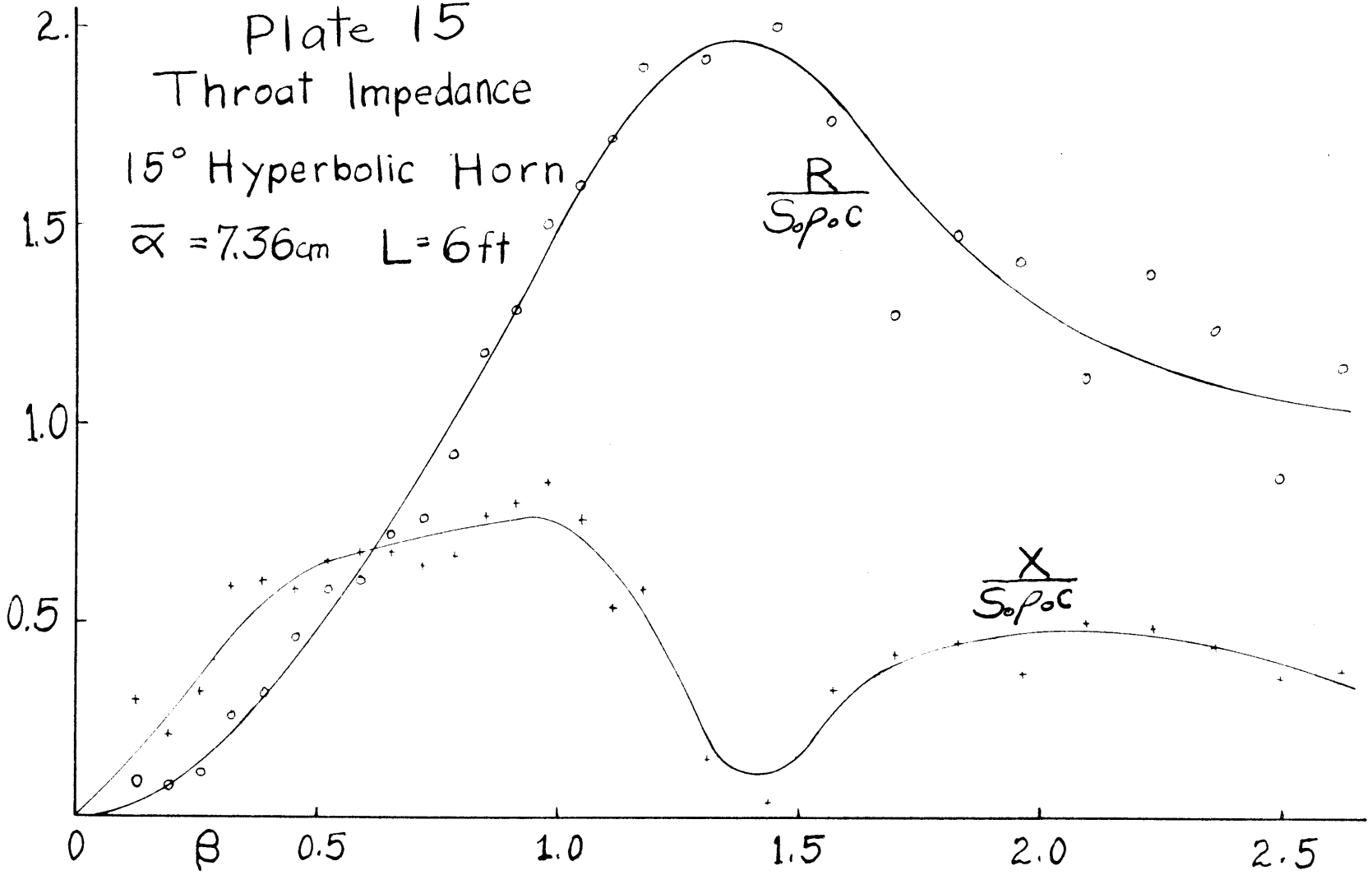
Plate 15
Throat Impedance
15° Hyperbolic Horn
$\bar{\alpha}$ = 7.36cm L = 6ft
$\frac{R}{S_0\rho_0 c}$
$\frac{X}{S_0\rho_0 c}$
2.
1.5
1.0
0.5
0
β
0.5
1.0
1.5
2.0
2.5

a maximum above the ultimate value, and the asymptotic drop down to it as β increases further. The shape differs from that of the theoretical curve (rough calculation communicated privately by Freehafer) in that the experimental peak is about 40% higher, and occurs at a frequency parameter β also approximately 40% higher. At the lowest frequencies the exact theory predicts a large slope which becomes infinite at the origin while from experiment the resistance tails into the origin with practically zero slope. All these discrepancies are no doubt due to the finiteness of the horn, which again introduces the complicating reflected wave, especially at low frequencies. However, the general shape is that predicted.

The reactance curve required more arbitrary smoothing than the resistance, as evinced by the scattering of the experimental points. Although no data from the exact theory was available, the values from a rough plane wave analysis should show no large peaks, which is borne out by the curve. Moreover, the dip in the reactance at the resistance maximum definitely agrees with measurements on other horns, and with the curves from plane wave theory[14].

For another check, the values of the impedance at the throat were calculated from the plane wave theory. The constants ψ_0 and φ_0 were found by assuming the mouth replaced by a piston of equal area, and the value of the radiation impedance at the mouth read off from Plate 1 and

Plate 16

Throat Impedance Comparison

Overall Dimensions Same

$d_t = 3/4"$ $d_m = 36"$ $L = 6'$

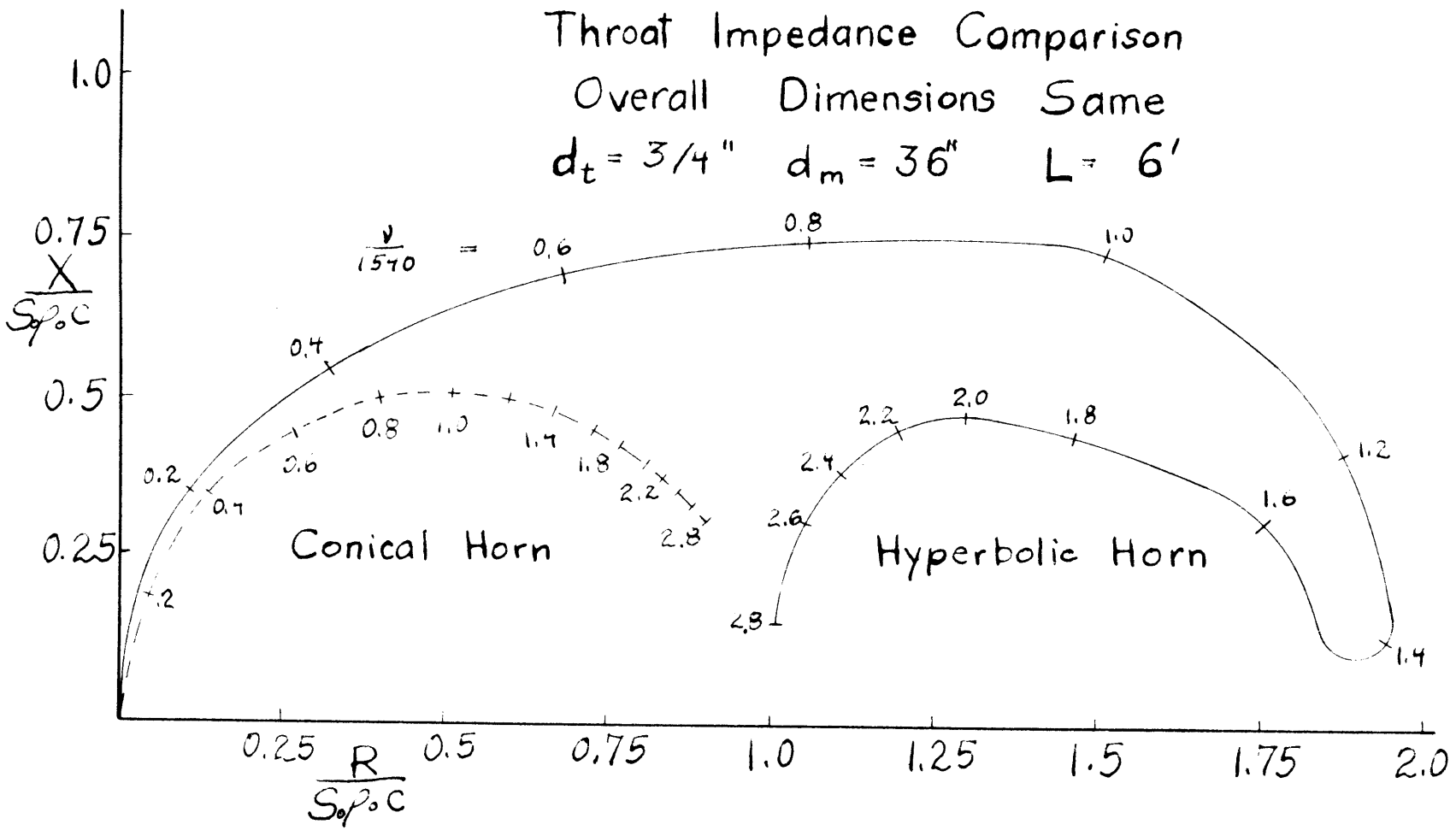

the constants evaluated. The table below shows the comparison of the calculations(at the four values of β^2 chosen) with the unsmoothed experimental values.

Comparison of Plane Wave Analysis and Experiment

Throat Impedance $Z/S_0\rho_0 c = r + jx$

β^2	.25		.5		1		2	
	r	x	r	x	r	x	r	x
Theory	.40	.73	.78	.89	1.19	.71	1.26	.29
Exp.	.52	.63	.75	.65	1.54	.82	1.96	.07

The agreement is only approximate, but is best at the lower frequencies, where the surfaces of equal amplitude and phase approach those of the plane type, as mentioned in the discussion of the field plots. Still, a fair estimate of the performance may be obtained by the plane wave theory; and since it is usually the low frequency performance which is of greatest interest, the analysis happily turns out to be of greatest aid where it best represents actual conditions.

For comparison with the conical horn, Plate 16 shows smoothed impedance loci for the two shapes. For the conical horn of the same overall dimensions, the locus from smoothed plane wave theory[14] is a semicircle centered at $(\frac{1}{2}, 0)$. Frequency is denoted by the marks on the loci, and by means of this,comparison is readily made. First, at the lowest frequencies the hyperbolic horn has practically twice the

impedance, at the same power factor or lag angle as the conical horn. Thus if the driving system is of the usual mass controlled moving coil type, the effective electrical reactance will depend but little on the acoustical reactance, so the larger radiation resistance of the hyperbolic horn will tend to increase the overall efficiency. However, since at very low frequencies the driver is hardly mass controlled, and the mouth impedance has considerable reactance, the gain will certainly be less than the two to one impedance ratio.

Next, at higher frequencies, the resistance peak in the hyperbolic horn may be sharp enough to be quite noticeable by the ear, although again the mouth conditions may be so adjusted that when its impedance is "reflected" to the throat, the effect at the piston is reduced. Any exact calculation to obtain the practical effect will be complicated by the variation of driver parameters with frequency, but the qualitative results cannot be far off from those suggested above.

On Plate 16, the exponential horn of the same overall dimensions yields a smoothed locus consisting of the $X/S_o\rho_o c$ axis from the origin to unity, and then a quarter circle (centered at the origin) ending at the ultimate point (1,0). For the dimensions given, the point corresponding to $(\nu/\nu_o) = (.1)$ occurs near the point $(\nu/\nu_o) = .6$ on the hyperbolic horn locus. Thus the exponential horn is already near its ultimate impedance, and hence should radiate low frequencies much more efficiently than either of the other types.

From this we may conclude that the order of increasing efficiency with an electromagnetic driver should be conical, hyperbolic and exponential horns. It should also be noted that this is the reverse order of ease of construction, and perhaps of initial cost.

VI SUMMARY

As far as agreement with theory goes, the results indicate that the experimental requirements for simulating an infinite horn demand the complete elimination of the reflected wave arising both from the abruptness of the mouth termination, and from incomplete absorption in the terminating space. Unless this requirement is met, exact quantitative agreement is not possible, but nevertheless the general features of the field may be correctly predicted. Qualitatively the plane wave analysis has been shown to yield results of sufficient accuracy to permit a knowledge of the gross behaviour. Using the throat impedance as a measure of the performance, the experimental results agree with exact and plane wave theory in demonstrating that the hyperbolic horn is slightly better than the conical, but that the exponential type still remains the best to construct from a given practical set of overall dimensions.

VII BIBLIOGRAPHY

1. Freehafer: "The Velocity Potential of an Hyperbolic Horn". M.I.T. Physics Thesis, 1936.

2. Rayleigh: "Theory of Sound" Section 244 (McMillan, 1878).

3. Crandall: "Theory of Vibrating Systems and Sound" Section 42 (VanNostrand, 1927).

4. Schelkunoff: "The Impedance Concept" BSTJ 17, 17(1938).

5. Eisenhart: "Separable Systems of Stäckel" Ann. Math. 35, 284 (1934).

6. Rayleigh, loc. cit. Ch. 17.

7. Webster: "Acoustic Impedance, and the Theory of Horns and of the Phonograph", PNAS 5, 275 (1919).

8. Morse: "Vibration and Sound" Section 22. (McGraw-Hill, 1936).

9. Morse, loc. cit. Section 24.

10. Crandall, loc. cit. Section 44.

11. Crandall, loc. cit. Section 46.

12. McLachlan: "Loudspeakers" Page 59 et seq. (Oxford, 1934).

13. Fay and Hall: "The Determination of the Acoustical Output of a Telephone Receiver from Input Measurements", JASA 5, 46 (1933).

14. Morse, loc. cit. Section 24.

15. Hartree: "A Practical Method for the Numerical Solution of Differential Equations", Memoirs and Proceedings of the Manchester Literary and Philosophical Society 77, 91 (1933).

APPENDICES

APPENDIX A.

Modified Hartree Method.

In many cases the wave equation is found to have the essential behaviour of the dependent variable stated in an equation of the form

$$f'' + Bf = 0,$$

where B is a specified function of the independent variable α. In many cases the solution is known for extreme values of α; and the purpose of the Hartree method is to allow the numerical evaluation of f at other points.

We shall not go into the details of the method in its most precise application, as that is completely set forth in reference 15, but shall merely derive a simple recursion formula which needs two known values of f to start. Suppose that the functions f and f'' have been arranged at equal increments $(\delta\alpha)$ of the independent variable. Then by successive differencing of the functions, the k^{th} difference at the position (in the table) n may be obtained as $\delta^k f_n$. Hartree's fundamental formula may be written as

$$\delta^2 f_n = (\delta\alpha)^2 \left[f_n'' + \frac{1}{12}\delta^2 f_n'' - \frac{1}{240}\delta^4 f_n'' + \cdots \right]$$

In general, $\delta^k f$ will need $(k + 1)$ values of f in order to be evaluated; hence if two starting points are to be used, the $\delta^4 f_n''$ term on the right must be omitted. It will be found that to any desired accuracy this is

possible if $(\delta\alpha)$ is small enough, which may be tested directly by observing the effect of doubling $(\delta\alpha)$, etc. Usually, if $dB/d\alpha$ is not large anywhere, then a single value of $(\delta\alpha)$ will suffice over the whole range.

With this provision we set

$$\delta^2 f_n = (\delta\alpha)^2 \left(f_n'' + \tfrac{1}{12}\delta^2 f_n'' \right)$$

Using $\delta f_{n+\frac{1}{2}} \equiv f_{n+1} - f_{n-1}$,

$$f_{n+1} - 2f_n + f_{n-1} = (\delta\alpha)^2 \left[f_n'' + \tfrac{1}{12}\left(f_{n+1}'' - 2f_n'' + f_{n-1}'' \right) \right]$$

Substituting $f'' = -Bf$, and solving for f_{n+1} we get

$$f_{n+1} = \frac{f_n\left[2 - \frac{(\delta\alpha)^2 B_n}{12}\right] - f_{n-1}\left[1 - \frac{(\delta\alpha)^2 B_{n-1}}{12}\right]}{\left[1 - \frac{(\delta\alpha)^2 B_{n+1}}{12}\right]}$$

If we now set $N \equiv \frac{12}{(\delta\alpha)^2}$ there results

$$f_{n+1} = \frac{f_n[2N - 10B_n] - f_{n-1}[N + B_{n-1}]}{[N + B_{n+1}]}$$

This has been used in the following tabular form suitable for calculation.

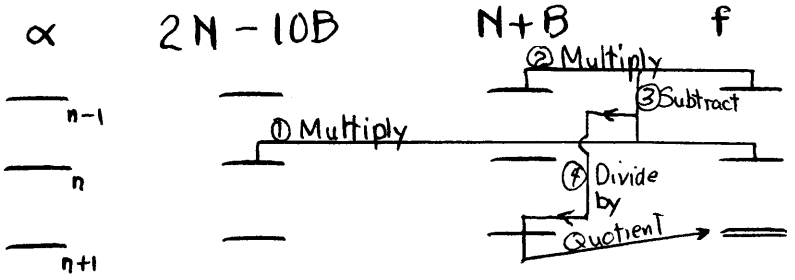

By using a calculating machine, and performing the operations in the order indicated f may be read directly off the quotient dial.

For obtaining derivatives there may be used

$$f_n' = \frac{f_{n+1} - f_{n-1}}{2(\delta\alpha)} + \frac{\delta\alpha}{12}\left(B_{n+1}f_{n+1} - B_{n-1}f_{n-1}\right)$$

which is adapted from equation (8) in Hartree's paper.

APPENDIX B.

Table of values of f

The following table lists solutions of the f equation for the hyperbolic horn

$$f'' + \left[\beta^2 - \frac{1}{(1+\alpha^2)^2}\right] f = 0$$

in the form

$$f = u - jv,$$

as obtained by the Hartree method described in Appendix A. The known values of f were obtained by

$$f \simeq e^{-j\beta\alpha}$$

at values of α large enough so that

$$\frac{1}{\beta^2(1+\alpha^2)^2}$$

was less than 1 % at the position of matching. The $(\delta\alpha)$ was -.05 for all but the last values for $\beta^2 = .25$. The values of u and v so obtained were used in the calculation of the pressure on the axis, and of the throat impedance.

The tables stop at such a value of α that the approximation $f \simeq e^{-j\beta\alpha}$ holds beyond that.

Values of u and v for hyperbolic horn equation.

	β^2 = .25		.5		1		2	
α	u	v	u	v	u	v	u	v
0	1.373	.244	1.298	.265	1.244	.260	1.130	.232
.2	1.234	.292	1.170	.348	1.117	.400	1.008	.456
.4	1.128	.348	1.061	.437	.986	.537	.844	.660
.6	1.045	.411	.962	.530	.844	.670	.637	.830
.8	.973	.478	.866	.623	.688	.789	.394	.952
1.0	.907	.548	.765	.714	.523	.889	.125	1.013
1.2	.841	.618	.657	.797	.343	.963	-.152	1.003
1.4	.772	.686	.540	.870	.151	1.004	-.418	.920
1.6	.698	.750	.415	.929	-.046	1.010	-.652	.768
1.8	.620	.809	.283	.973	-.241	.979	-.837	.558
2.0	.537	.861	.146	1.000	-.427	.912	-.957	.305
2.2	.449	.907	.006	1.008	-.597	.809	-1.002	.028
2.4	.357	.944	-.134	.998	-.744	.675	-.969	-.252
2.6	.262	.973	-.271	.968	-.861	.514	-.860	-.511
2.8	.165	.993	-.403	.919	-.945	.334	-.683	-.730
3.0	.066	1.003	-.528	.853	-.992	.140	-.452	-.892
3.2	-.034	1.004	-.642	.770	-.999	.059		
3.4	-.133	.995	-.743	.672	-.967	-.256		
3.6	-.231	.976	-.829	.561	-.897	-.443		
3.8	-.327	.948	-.900	.438	-.791	-.612		
4.0	-.419	.911	-.952	.307	-.654	-.757		
4.2	-.507	.864	-.986	.170				
4.4	-.591	.809	-1.000	.030				
4.6	-.668	.746	-.994	-.111				
4.8	-.739	.676	-.968	-.250				
5.0	-.802	.599	-.923	-.384				
5.2	-.858	.515						
5.4	-.905	.427						
5.6	-.943	.335						
5.8	-.971	.239						
6.0	-.990	.141						
6.2	-.999	.042						
6.4	-.998	-.058						
6.6	-.988	-.158						
6.8	-.967	-.256						
7.0	-.936	-.351						

BIOGRAPHICAL NOTE

The author's university training began at Temple University, from which he received a B.A. in 1934. A two year Teaching Fellowship led to an M.A. in Physics in 1936, from the same institution. He entered the Graduate School of the Massachusetts Institute of Technology in the same year with the aid of a half scholarship, continued through the second year with a Teaching Fellowship in Physics, and finished with a half year full scholarship. He is a member of the Physical Society of London and has combined a great deal of Electrical Communications Engineering with the study of pure Physics.